NASA TECHNICAL NOTE

NASA TN D-3162

NASA TN D-3162

STRUCTURAL CONCEPTS FOR HYDROGEN-FUELED HYPERSONIC AIRPLANES

by L. Robert Jackson, John G. Davis, Jr., and Gregory R. Wichorek

Langley Research Center
Langley Station, Hampton, Va.

NATIONAL AERONAUTICS AND SPACE ADMINISTRATION • WASHINGTON, D. C. • FEBRUARY 1966

NASA TN D-3162

STRUCTURAL CONCEPTS FOR HYDROGEN-FUELED HYPERSONIC AIRPLANES

By L. Robert Jackson, John G. Davis, Jr.,
and Gregory R. Wichorek

Langley Research Center
Langley Station, Hampton, Va.

NATIONAL AERONAUTICS AND SPACE ADMINISTRATION

For sale by the Clearinghouse for Federal Scientific and Technical Information
Springfield, Virginia 22151 – Price $2.00

STRUCTURAL CONCEPTS FOR HYDROGEN-FUELED HYPERSONIC AIRPLANES

By L. Robert Jackson, John G. Davis, Jr.,
and Gregory R. Wichorek
Langley Research Center

SUMMARY

Two structural concepts have been identified and investigated to obtain a better insight into problems associated with structures for hydrogen-fueled hypersonic airplanes. One of these is the multiwall sandwich concept which combines the evacuated thermal protection, tankage, and load-carrying functions into a single component. The other concept is based on the use of an unsealed structure that does not require vacuum sealing, but rather utilizes carbon dioxide gas to purge the insulation space between the structure and tanks. A brief look at some characteristics of these two concepts and some analytical and experimental results related to the concepts are presented.

INTRODUCTION

In recent years considerable interest has developed in hydrogen-fueled hypersonic airplanes, and some studies of such vehicles have been made. (For example, see refs. 1 and 2.) Such airplanes pose many interesting and difficult structures and materials problems. The structure of such vehicles must contain large volumes of fuel and will consequently be large. Large temperature differences resulting from surface temperatures that range from -423° F (20.4° K) (the boiling point temperature of liquid hydrogen (H_2)) to perhaps 2400° F (1590° K) at the external surface will pose severe thermal stress and insulation problems. In order that such airplanes be effective, a low unit-mass of the structure is required. Efficient and low mass thermal protection systems are required to prevent excessive vaporization of the fuel. In addition, the thermal protection system must prevent cryogenic pumping of air to the liquid H_2 tank walls. The high temperature associated with the external surfaces will probably require frequent replacement or refurbishment of portions of the structure.

In order to obtain some insight into the structures and materials problems common to hydrogen-fueled hypersonic airplanes, studies are underway at the Langley Research Center to establish structural concepts that appear particularly useful for such airplanes. Two promising structural concepts that have been selected for detailed study are

described herein. The analytical and experimental studies related to these concepts are presented. A preliminary estimate of the mass of each concept is included in which primary attention was devoted to fuselage structure; in addition, calculations for typical points on the wing are included.

SYMBOLS

The units used for the physical quantities defined in this paper are given both in U.S. Customary Units and the International System of Units (SI) (ref. 3). Appendix A presents factors relating these two systems of units.

A	fractional area of metallic conduction
b	plate width, in. (cm)
c_p	specific heat, Btu/lbm-^oR (J/kg-^oK)
d	depth of dimpled core sheet, in. (cm)
E	modulus of elasticity, psi (N/m^2)
F	configuration factor
f	view factor
G	shear modulus of elasticity, psi (N/m^2)
$g(M_{ins})$	function of insulation mass, defined by equation (2)
H	convective heat transfer coefficient, Btu/hr-ft^2-^oR (W/m^2-^oK)
H_r	radiant heat transfer coefficient, Btu/hr-ft^2-^oR (W/m^2-^oK)
h	sandwich thickness, in. (cm)
Δh	enthalpy change, Btu/lbm (J/kg)
j	total number of sheets or radiation barriers
K_x	plate buckling coefficient
k	thermal conductivity, Btu/hr-ft-^oR (W/m-^oK)
L	thickness, ft (m)
M	unit-area mass, lbm/ft^2 (kg/m^2)

N_x	compressive buckling load per unit circumference in the longitudinal direction, lbf/in. (N/m)
n	total number of dimpled core sheets in structural portion of multiwall sandwich
P_i	compressive load per unit width, lbf/in. (N/m)
p	dimple pitch or cell width, in. (cm)
Q	heat load, Btu/ft^2 (J/m^2)
R	cylinder radius, in. (cm)
r	defined by equation (B9)
T	temperature, ^oR (^oK)
t	thickness, in. (cm)
$\bar{t}$	cross-section area of sandwich per unit width expressed as an equivalent thickness, in. (cm)
X	coordinate, ft (m)
Z	conduction path length, ft (m)
z	total thickness of metal measured normal to the sandwich surface, ft (m)
α	sandwich core shear stiffness parameter
β	cube of ratio of mean temperature to average temperature of sandwich
ϵ	emittance
η	plasticity reduction factor
λ	ratio of time that frost is being expended to the powered phase of ascent flight time
μ	Poisson's ratio
ρ	density, lbm/ft^3 (kg/m^3)
σ	stress, psi (N/m^2); or Stefan-Boltzmann constant, 1.713×10^{-9} $Btu/ft^2\text{-hr-}^oR^4$ ($56.7\ nW/m^2\text{-}^oK^4$)
τ	powered phase of ascent flight time, hr
ϕ	defined by equation (B7)

Subscripts:

a	apparent
ave	average
C	cold face
c	core or coolant
cy	compressive yield
F	frost
f	final or face sheet
fu	fuel
G	ground hold conditions
g	gas
H	hot face
I	initial
ins	insulation
m	metal
o	outer surface
p	panel
s	sublimation
t	tank
tp	thermal protection
v	vaporization
1	initial hot face of frost
2	final hot face of frost

Primed symbols indicate quantities evaluated during the interval from the time the frost has been expended until the end of the powered phase of ascent flight.

DESCRIPTION OF STRUCTURAL CONCEPTS

Several different structural designs for the tankage areas of hydrogen-fueled airplanes were studied in order to define the more promising concepts. Two of these concepts are identified and described in the following sections, and the related analysis and experimental efforts are presented.

Multiwall-Sandwich Structure

The multiwall-sandwich structure concept, hereinafter designated as the multiwall concept, is shown in figure 1. This design consists of layers of dimpled and flat sheets welded at the crests of dimpled sheets to form a sandwich. The sealed outer skin is thin-gage sheet and is lightly dimpled to induce out-of-plane deformation at low thermal in-plane loads.

Polished foils with evacuated spaces serve as the thermal protection. Pressure loads are transmitted through the insulating layers to the inner structural portion of the sandwich with negligible deformation normal to the insulating layers. The structural portion of the sandwich supports in-plane loads and serves as the liquid H_2 tank wall.

Structural sheets may be a titanium alloy. Additional insulating layers of corrosion-resistant steel may be added inside the titanium structural layers for oxygen (O_2) tankage. The outer insulating layers may be titanium and nickel-base alloys, and refurbishable multiwall sandwich shields of coated refractory metals may be fastened to the outer skin shown in figure 1.

The multiwall sandwich may be fabricated from several metals without having to weld dissimilar metals. A mechanical interlocking of dissimilar metals is accomplished by a bimetal layer as shown in figure 1. The bimetal layer is formed by simultaneous dimpling of a sheet of each metal. One metal thickness is removed from each side of the bimetal layer at the dimpled crests thereby exposing similar metal for welding to adjacent layers.

The integration of thermal protection, structural, and tankage functions into a single sandwich panel concept results in low unit mass. However, the low mass of this design is perhaps offset by the complex fabrication problems. The multiplicity of welds in thin sheet utilized in this design leads to potential leaks that may adversely affect the vacuum retention required for low thermal conductance, for protection of the foil from oxidation, and for prevention of cryogenic pumping.

Carbon Dioxide Concept

The carbon dioxide concept is shown in figure 2. In this design the functions of load-carrying structure, thermal protection, and tankage are performed by separate

components. Sufficient aerodynamic heating causes sublimation of the carbon dioxide (CO_2) frost that was deposited within the insulation on the tankage walls during ground hold; the space between the primary structure and tankage is purged with the resulting CO_2 gas. The CO_2 gas pressure is sufficient to prevent the entrance of air through the unsealed primary structure.

Before tank cool-down the space between the structure and tanks is purged of air by He gas. When any portion of the tank wall is cooled during ground-hold time to about -110° F (194° K), CO_2 gas is introduced into the helium atmosphere. Some of the CO_2 gas solidifies as a frost within the voids of the fibrous insulation on the tankage walls. When the required amount of CO_2 frost is deposited, the CO_2 gas supply is stopped and purging is continued with only He during the remainder of the ground-hold period and the early flight period. The deposit of frost sublimes during flight, thereby blocking heat transfer to the fuel and providing a supply of purge gas. It may be necessary to heat the purge gases during ground hold to prevent freezing of water vapor on aerodynamic surfaces.

The density of the frost-insulation composite should be as low as possible to maintain low thermal conductivity and low gross mass; however, the density must be sufficient to resist the entrance of additional CO_2 gas into the frost after sublimation of the frost starts. The density at which CO_2 frost is deposited is affected principally by the presence and pressure of the He gas, by the partial pressure of the CO_2 in the He surrounding the insulation, and by the rate of heat removal from the hot face of the frost deposit.

Analyses supported by preliminary test results indicate that the carbon dioxide concept offers the potential for obtaining a structure with an acceptable mass. The fabrication of this structural concept appears to be within the present state of the art. A possible deficiency is that considerable time (approximately 8 hr/in. (3 hr/cm)) will be required for deposition of the required amount of CO_2 frost – usually about 3/8 in. (1 cm).

METHODS OF ANALYSES

Primary attention was directed at fuselage structure in the preliminary unit-mass analyses; however, calculations for typical points on the wing were also made for the multiwall concept and for a modified carbon dioxide concept to be discussed later. To obtain an estimate of unit-area mass for either the multiwall concept or the carbon dioxide concept, it was necessary to assume configurations, load factors, and trajectories. The configurations considered for the structural concepts were large winged bodies with a delta-planform wing. The trajectories used for the multiwall sandwich analyses are shown in figures 3 and 4, and the trajectories used for the carbon dioxide concept analyses are shown in figure 5. Trajectory analyses were performed with a numerical analysis program. This program calculated trajectory data based on the two-dimensional equations

of motion. Details of the mass analyses are beyond the scope of this paper; however, the bases for the analyses are presented in this section of the paper.

Structural Analyses

Multiwall concept.- The approximate masses of the structure at four points were determined from loads and temperatures associated with the assumed trajectories. Inertial, thrust, and air loads were computed with data obtained from the trajectory analysis. The method presented in reference 4 was used to determine the air loads. Internal pressure was assumed constant at 10 psig (68.9 kN/m2), and thermal loads were calculated with the use of surface temperatures shown in figures 6 and 7. The largest net load with load factors applied to each load was used to estimate the loading intensities and then to obtain the mass of the structure.

Estimates of the mass of multiwall sandwich cylinders were made with equations presented in appendix B. The structural index curve based on these equations is shown in figure 8. As indicated in figure 8 for the range of structural indexes utilized in this study, the multiwall sandwich is approximately as efficient as other more familiar types of sandwich for cylinders in edge compression. Curves for other structures are shown in figure 8 for comparison. The curves for unstiffened, Z-stiffened, and truss-core sandwich cylinders were taken from reference 5. The curve for the waffle stiffened cylinder was taken from reference 6. The solid portion of the curve for the honeycomb-core sandwich cylinder was calculated with the use of the equations presented in appendix B, and the dashed portion of the curve was faired to approach the E/σ_{cy} curve asymptotically. Material properties of a titanium alloy (Ti-6Al-4V) were used in the preliminary mass analysis of the primary structure of the multiwall concept. The primary structure mass was computed for four points on the airplane to examine conditions at different locations. The structural index calculated to estimate the mass of the primary structure in the fuselage was 8.5×10^{-7}, which corresponds to a buckling load of about 1600 lbf/in. (280 kN/m).

The primary structure mass estimate for the wing panels was affected principally by internal pressure loading since the wing of the vehicle selected for multiwall concept analyses contained fuel. However, the panels were also subjected to edge compression loads. Loads caused by bending are 310 lbf/in. (54.7 kN/m) for spanwise edge compression and 1900 lbf/in. (333 kN/m) for chordwise edge compression at the point selected on the upper surface of the wing. Structural index curves for flat plates are shown in figure 9. The curve for multiwall sandwich was calculated from the equations presented in appendix B. The solid portion of the curve for honeycomb-core sandwich was calculated from equations in appendix B, and the dashed portion of this curve was taken from reference 7. The curves for the other types of structure were taken from reference 5, in which for high structural indexes these curves were faired to approach the E/σ_{cy} line asymptotically.

Carbon dioxide concept.- To calculate an approximate unit-area mass of a fuselage section an edge compression load at buckling of 2000 lbf/in. (350 kN/m) was assumed. This value was selected intentionally to be greater than the 1600 lbf/in. (280 kN/m) buckling load calculated for the multiwall concept, which had a more severe trajectory, because a conservative estimate of the mass was desired. The estimated mass was based on local buckling of all flat elements of the Z-stiffeners equal to local buckling of the skin where plate buckling coefficients were estimated from literature for similar elements. Proportions and pitch of Z-stiffeners and the skin gage were varied to obtain a maximum ratio of radius of gyration to column area per unit width. The calculated mass was based on Euler's buckling equation with an assumed wide-column fixity factor of 2.0.

Material properties of a nickel-base alloy (René 41) were used in computing the preliminary mass of the primary structure. Preliminary temperature analysis indicated that the peak temperature, shown in figure 10, is in the usable range of nickel-base alloys.

The estimate of the mass of the waffle-plate tank was based on an assumed internal pressure of 40 psig (276 kN/m^2) with a safety factor of 2.0 between the pressure load stress and burst stress. The waffle proportions were sized, with the data from reference 6, to support an edge compressive load of 1000 lbf/in. (175 kN/m). This load was selected to support the fuel mass in an unpressurized tank.

Material properties of an aluminum alloy (2219-T6) were used in estimating the mass of the tank. On the upper surface of the tank, more insulation and frost than that required for minimum thermal protection was used in the analysis to limit the tank temperature to 70° F (294° K) (fig. 10) so that an aluminum alloy could be selected.

Thermal Protection Analyses

Multiwall concept.- In calculating approximate mass of the thermal protection material, a numerical analysis program was used. This program calculates both aerodynamic heating by the method of Van Driest and the temperature distribution through the wall by a numerical solution to Fourier's equation for one-dimensional unsteady-state heat conduction. The wall thickness was incremented and numbered as shown in figure 1, and the innermost increment, increment 11, represented the fuel. Material properties for increment 11 were selected to result in a negligible temperature rise to be consistent with the constant temperature fuel. Material properties of the increment adjacent to the fuel, increment 10, were calculated to represent heat transfer coefficients for either the boiling fuel or radiation through the tank pressurizing gas. Heat load to the fuel was obtained by graphical integration of the heat rate into increment 10. Calculations for several thicknesses of insulation were performed to relate the fuel heat load to the insulation mass. A second-order best-fit equation, computed by the method of least squares, was obtained for this relationship and used in determining the minimum thermal protection

mass. The thermal protection mass M_{tp} equals the sum of vaporized fuel mass M_{fu} and the insulation mass M_{ins} or

$$M_{tp} = M_{fu} + M_{ins} \tag{1}$$

where

$$M_{fu} = \frac{Q_{fu}}{\Delta h_{fu}} = \frac{g(M_{ins})}{\Delta h_{fu}} \tag{2}$$

in which $g(M_{ins})$ is the best-fit expression for the heat load that transferred to the fuel Q_{fu} during time τ in terms of M_{ins}. Equation (1) is minimized with respect to M_{ins} after substitution of equation (2) for M_{fu}. The expression $g(M_{ins})$ is a continuous function; however, the insulation consists of discrete layers. Therefore, the minimum mass thermal protection is the sum of the masses of that number of insulating layers and the corresponding vaporized fuel that more nearly equals the minimum of equation (1).

A plot of equation (1) is shown in figure 11. The mass of a refurbishable heat shield is included in the insulation mass curve shown in figure 11. The mass curve for vaporizing fuel shown in figure 11 is based on a saturated liquid with a constant heat of vaporization. As indicated in figure 11, the use of less insulation than the amount required for minimum thermal protection mass does not result in a severe mass penalty.

The apparent thermal conductivity of each dimpled layer of the multiwall sandwich was used in the preceding calculations. The equation used to calculate apparent thermal conductivity is presented in appendix C. This equation includes metal conduction, gaseous conduction or convection, and radiation through the sandwich. The spaces between the insulating layers were assumed to be evacuated to 10^{-5} torr (1.3 mN/m^2) or less, and the core space of the structural portion of the sandwich was assumed to be pressurized lightly with He. For inner insulating layers properties of a titanium alloy (Ti-6Al-4V) were used in the analyses, and for the outer layers the properties of a nickel-base alloy (René 41) were used. The refurbishable shield, of multiwall sandwich, was analyzed on the basis of columbium alloy (Cb-10Ti-5Zr) properties.

Carbon dioxide concept.- In calculating approximate thermal protection mass, the equations presented in appendix C were used. These equations include the mass of insulation, CO_2 frost, and vaporized fuel. To obtain the average aerodynamic surface temperature T_o, a thin-skin analysis was performed by a numerical analysis program. The fractional location of the initial hot face of the frost x_1/L was calculated by a steady-state heat transfer analysis based on ground-hold conditions in which the hot-face temperature of the insulation was assumed to be 70^o F (294^o K) and in which the deposition of CO_2 frost was permitted until equilibrium conditions were approached through the lower fuselage wall. Mass calculations for the lower fuselage thermal protection were based on the assumption that fuel remained in contact with the tank only during the powered phase

of the ascent flight time. Mass calculations for the upper fuselage thermal protection were based on the assumption that fuel contact with the tank ceased at take-off. The constraints on the calculation were that the upper tank temperature would be -160° F (167° K) at the end of powered ascent flight and that the initial frost thickness on the upper tank surface would be equal to the initial frost thickness on the lower tank surface. Therefore, the thickness of insulation was calculated to result in a tank temperature of -160° F (167° K). With this thickness a finite difference calculation was performed to determine the maximum tank temperature during return glide. As indicated in figure 10, the upper surface tank temperature remained below 70° F (294° K). A similar calculation for the lower surface, based on minimum mass thermal protection for powered ascent flight, indicates that a maximum tank temperature of less than 70° F (294° K) was maintained during return glide (fig. 10).

RESULTS AND DISCUSSION

Analytical Results

Approximate unit-area masses for the multiwall structural concepts are tabulated in table I(a). The mass of the primary structure for the fuselage includes an estimated 1.0 lbm/ft^2 (4.88 kg/m^2) for internal structure. Estimates of side structural panel and erosion shield masses and wetted area distributions indicate that the average structure mass would be somewhat less than that tabulated for the upper and lower body. Tabulated wing masses of the primary structure include an allowance of 1.2 lbm/ft^2 (5.86 kg/m^2) for rib and spar masses.

Approximate unit-area masses for the carbon dioxide concept are tabulated in table I(b). The mass of the primary structure includes an estimated 1.0 lbm/ft^2 (4.88 kg/m^2) for the internal structure. The frost mass is that charged to thermal protection mass. This mass includes half the mass of frost sublimed during ascent flight and all the mass of frost sublimed during return glide. Half the mass of frost sublimed during ascent is charged to thermal protection because this represents the average mass of frost sublimed during ascent that was carried throughout powered flight since the gas resulting from sublimation is continuously vented from the airplane.

To compare the multiwall concept masses to the carbon dioxide concept masses, a modified carbon dioxide concept, shown in figure 12, was analyzed for the same configuration, load factors, and trajectories as the multiwall concept. The modified carbon dioxide concept consists of an insulated integral-tankage structure where erosion shields are fastened through panels of fibrous insulation to a primary structure of truss-core sandwich. The analytical procedure used for estimating masses for the primary structure of this concept was the same as for the multiwall concept. However, the material properties

of a nickel-base alloy (René 41) were used for the primary structure mass estimates. The equations in appendix C were used to estimate thermal protection mass. Approximate unit-area masses for this modified carbon dioxide concept are tabulated in table I(c), and the values for the multiwall sandwich concept from table I(a) may be compared with values in table I(c). The same allowance for internal structure mass was made for the fuselage of this modified carbon dioxide concept as for the multiwall concept, but an added 0.2 lbm/ft^2 (0.98 kg/m^2) was used for the wing internal structure mass in the modified carbon dioxide concept because the sandwich requires strengthening transverse to the corrugations.

The fractional location of the initial hot face of the frost at both lower and upper surfaces was that value obtained by permitting deposition until equilibrium conditions were approached during ground hold. The assumptions made regarding fuel contact with the tank were the same as those made for the carbon dioxide concept. The CO_2 frost mass for the lower surface includes half the mass of frost sublimed during powered flight plus the mass of frost remaining at the end of powered flight. For the upper surface the frost mass is half the mass sublimed during powered flight times the ratio of time that frost remained on the tank wall to the time of powered flight. This ratio λ has a value less than unity since, on the upper tank surface, analysis indicated that all frost sublimed before the end of powered flight.

Experimental Results

Multiwall concept.- Multiwall sandwich panels fabricated from type 301 stainless steel were tested to determine thermal conductivity and to obtain some insight into performance under thermal cycling and exposure to random noise. A typical panel is shown in figure 13.

Two 1- by 12- by 12-inch (2.5- by 30.5- by 30.5-cm) panels (fig. 13) were tested to determine thermal conductivity and to verify the apparent thermal conductivity analyses performed on this concept. The panels were tested at average temperatures ranging from about 500 to 2000° F (530 to 1370° K); the edges of the panels were open and exposed to room air. The test results were compared with calculated values from the equation (C1) in appendix C. The details of the experiments are reported in appendix D. The experiments indicate reasonable agreement with the calculated values as shown in figure 14.

One multiwall panel, such as shown in figure 13, was subjected to thermal cycling to investigate weld integrity and to test the design principle used for thermal expansion of the outer surface. The panel was supported on its four corners and subjected to cyclic radiant heating. The temperatures of the heated face ranged from about 250 to 1725° F (395 to 1210° K). The heating period was 2 minutes long. Other details of the experiment are given in appendix D. The experiment was inconclusive because the specimen tested

had been reworked to add an 0.008-in. (204-μm) thick lightly dimpled outer skin. The rework resulted in a mismatch of dimpled core layers causing inadequate welding of the new core sheet to the exposed core sheet of the original specimen. However, the outer face sheet remained intact with the core after the panel had experienced 25 cycles.

A noise test at room temperature was performed on a multiwall panel, 0.5 by 18 by 18 inches (1.27 by 45.7 by 45.7 cm), to determine the resistance of the welded construction to sonic fatigue. Edges of the panel were closed by a thin sheet that was fusion seam-welded to the face sheets. The panel was simply supported in the test apparatus. Other details of the experiment are presented in appendix D. After exposure to a random noise level of 162 decibels for 90 minutes, visual inspection of the panel indicated no damage.

Carbon dioxide concept.- At the outset of this study no data were available on thermal conductivity of CO_2 frost. Therfore, to obtain the data necessary to analyze the carbon dioxide concept, tests were performed to establish the thermal conductivity of CO_2 frost and the feasibility of deposition of CO_2 frost within the voids of a fibrous insulation.

Results of experiments to determine the apparent thermal conductivity of CO_2 frost cryodeposited at an average density of 29.5 lbm/ft^3 (473 kg/m^3) within the voids of a 4.0 lbm/ft^3 (64.1 kg/m^3) fibrous insulation are shown in figure 15 (from data supplied by General Dynamics, Astronautics Division, San Diego, California, under Contract NAS 1-4017). In addition, tests were performed to determine the conditions necessary for cryogenic deposition of CO_2 frost at a specific density. As indicated in appendix E, CO_2 frost at a density of approximately 30 lbm/ft^3 (481 kg/m^3) will form in fibrous insulation having a density of 6.5 lbm/ft^3 (104 kg/m^3) when the CO_2 gas flow rate is 3 ft^3/hr-ft^2 (254 cm^3/s-m2) of cooled tank-surface area. The CO_2 gas is introduced during tank cool-down into a helium atmosphere that is at a pressure of 1 psig (6.89 kN/m^2). The deposition rate for the CO_2 frost was about 0.12 in./hr (1 μm/s). Purging with only CO_2 during tank cool-down produced CO_2 ice at a density of about 100 lbm/ft^3 (1.6 Mg/m^3) within the voids of the fibrous insulation. Data obtained under contract indicated that after the removal of He with a noncondensing, nonsubliming frost a two-fold increase in frost density and conductivity occurred within 2 hours when only CO_2 was purged around a frost that had an average density of 29.5 lbm/ft^3 (473 kg/m^3) when cryodeposited within the voids of a 4.0 lbm/ft^3 (64.1 kg/m^3) fibrous insulation. However, it is not known that CO_2 gas resulting from frost sublimation will cryopump into a subliming frost. Therefore, additional experiments are necessary to determine whether or not CO_2 gas resulting from sublimation of the frost will cryopump into a subliming low density frost.

CONCLUDING REMARKS

This study of structural concepts for hydrogen-fueled hypersonic airplanes has led to two basic and different concepts. One concept is based on the use of a multiwall sandwich structure that consists of alternate layers of flat and dimpled sheets welded together. This concept combines evacuated thermal protection, tankage, and load-carrying functions in a single component. The design appears to be a possible solution to obtaining a very low unit-mass structure. The requirement of vacuum-tight construction coupled with the need for foil thickness materials makes this design difficult to fabricate and to maintain a leak proof structure. The other design is a carbon dioxide concept which utilizes an unsealed structure and prevents cryogenic pumping of air around liquid-hydrogen tanks during flight by the use of CO_2 gas that results from sublimation of CO_2 frost. This concept is generally heavier than the multiwall concept but appears to be simpler to fabricate and maintain. A possible deficiency of the carbon dioxide concept is that considerable time (8 hr/in. (3 hr/cm)) will be required to deposit the required amount – usually about 3/8 in. (1 cm) – of CO_2 frost within the voids of a fibrous insulation.

Langley Research Center,
National Aeronautics and Space Administration,
Langley Station, Hampton, Va., September 7, 1965.

APPENDIX A

CONVERSION OF U.S. CUSTOMARY UNITS TO SI UNITS

The International System of Units (SI) was adopted by the Eleventh General Conference on Weights and Measures, Paris, October 1960, in Resolution No. 12 (ref. 3). Conversion factors for the units used herein are given in the following table:

Physical quantity	U.S. Customary Unit	Conversion factor (*)	SI unit
Density	lbm/ft^3	16.02	kilograms per cubic meter (kg/m^3)
Enthalpy	Btu/lbm	2.324×10^3	joules per kilogram (J/kg)
Heat load	Btu/ft^2	1.136×10^4	joules per square meter (J/m^2)
Heat transfer coefficient	$Btu/hr\text{-}ft^2\text{-}^oR$	5.689	watts per square meter-degrees Kelvin ($W/m^2\text{-}^oK$)
Length	in.	0.0254	meters (m)
	ft	0.3048	meters (m)
Load per unit width	lbf/in.	175.1	newtons per meter (N/m)
Pressure	torr	133.3	newtons per square meter (N/m^2)
Specific heat	$Btu/lbm\text{-}^oR$	4.184×10^3	joules per kilogram-degrees Kelvin ($J/kg\text{-}^oK$)
Stress	$psi = lbf/in^2$	6.895×10^3	newtons per square meter (N/m^2)
Temperature	$(^oF + 459.67)$	5/9	degrees Kelvin (^oK)
Thermal conductivity	$Btu/hr\text{-}ft\text{-}^oR$	1.732	watts per meter-degrees Kelvin ($W/m\text{-}^oK$)
Unit mass	lbm/ft^2	4.882	kilograms per square meter (kg/m^2)

*Multiply value given in U.S. Customary Unit by conversion factor to obtain equivalent value in SI unit.

Prefixes to indicate multiple of units are as follows:

Prefix	Multiple
mega (M)	10^6
kilo (k)	10^3
hecto (h)	10^2
centi (c)	10^{-2}
milli (m)	10^{-3}
micro (μ)	10^{-6}
nano (n)	10^{-9}

APPENDIX B

MASS ANALYSIS OF MULTIWALL STRUCTURE

The preliminary mass analysis of the multiwall structure concept has been discussed in the body of this paper. This appendix presents the equations which were used to compute the required mass for the primary load-carrying portion of the multiwall sandwich. The equations for multiwall panels are derived from equation (2) in reference 8. The equations for multiwall cylinders are derived from equation (B9) in reference 9. General buckling is set equal to local buckling in the derivation for the panels and cylinders.

Multiwall Sandwich Panels

The structural index of the multiwall sandwich panels may be computed from

$$\frac{P_i}{b\eta E} = \frac{2\left(\frac{\sigma}{\eta}\frac{t_f}{h}\right)}{E\left(\frac{b}{h}\right)} \tag{B1}$$

and the corresponding equivalent thickness of material $\bar{t}$ is obtained from

$$\frac{\bar{t}}{b} = \frac{2 + \left(\frac{\rho_c}{\rho_f}\right)\left(\frac{h}{t_f} - 1\right)}{\left(\frac{h}{t_f}\right)\left(\frac{b}{h}\right)} \tag{B2}$$

The panel width to thickness ratio is computed from

$$\frac{b}{h} = \sqrt{\frac{\left(t_f/h\right)}{\phi}} \tag{B3}$$

where the ratio of panel thickness to face sheet thickness is given by

$$\frac{h}{t_f} = \sqrt{3\left[\frac{K_x}{3}\left(\frac{n}{r}\right)^2\left[\frac{\pi^2 E}{\left(1 - \mu^2\right)}\right]\right]\left[\frac{1}{\left(\frac{\sigma}{\eta}\right)\left(\frac{t_f}{h}\right)}\right]} \tag{B4}$$

in which

$$\frac{n}{r} = \frac{n}{p/d} \tag{B5}$$

and

APPENDIX B

$$\frac{\sigma}{\eta}\left(\frac{t_f}{h}\right) = \frac{\phi\pi^2 E/(1 - \mu^2)}{\left[1 + \dfrac{\pi^2\phi}{(1 - \mu)\alpha\left(\dfrac{\rho_c}{\rho_f}\right)}\right]^2} \tag{B6}$$

The dimensionless quantity ϕ is defined by

$$\phi = \frac{t_f h}{b^2} \tag{B7}$$

which is assumed throughout a range of values in calculating the structural index curve shown in figure 9; α is computed from

$$\alpha = \left(\frac{G_c}{G}\right)\left(\frac{\rho_f}{\rho_c}\right)\left(\frac{h}{h - t_f}\right) \tag{B8}$$

Honeycomb sandwich panel masses may be computed by using equations (B1) to (B8) when n is replaced by 1/2 and r is computed from

$$r = \frac{p}{h} \tag{B9}$$

Multiwall Sandwich Cylinders

The structural index of multiwall sandwich cylinders may be computed from

$$\frac{N_x}{R\eta E} = \frac{2}{\sqrt{1 - \mu^2}}\left(\frac{h}{R}\right)^2 \frac{t_f}{h}\left[1 - \left(\frac{t_f}{h}\right)\left(\frac{h}{R}\right)\left(\frac{1}{\alpha\dfrac{\rho_c}{\rho_f}}\right)\sqrt{\frac{1 + \mu}{1 - \mu}}\right] \tag{B10}$$

and the corresponding equivalent thickness of material $\bar{t}$ is obtained from

$$\frac{\bar{t}}{R} = \frac{2 + \left(\dfrac{\rho_c}{\rho_f}\right)\left(\dfrac{h}{t_f} - 1\right)}{\left(\dfrac{h}{t_f}\right)\left(\dfrac{R}{h}\right)} \tag{B11}$$

The panel thickness to face sheet thickness ratio is computed from

$$\frac{h}{t_f} = \frac{1}{2}\left(\frac{h}{R}\right)\left(\frac{1}{\alpha\dfrac{\rho_c}{\rho_f}}\right)\sqrt{\frac{1 + \mu}{1 - \mu}} + \frac{1}{2}\sqrt{\left(\frac{h}{R}\right)^2\left(\frac{1}{\alpha\dfrac{\rho_c}{\rho_f}}\right)^2\left(\frac{1 + \mu}{1 - \mu}\right) + \frac{4K_x}{3}\left(\frac{R}{h}\right)\left(\frac{n}{r}\right)^2 \frac{\pi^2}{\sqrt{1 - \mu^2}}} \tag{B12}$$

in which (n/r) and α are obtained from equations (B5) and (B8), respectively. The value of (h/R) is varied to obtain the multiwall structural index curve shown in figure 8.

Honeycomb sandwich cylinder masses may be computed by using equations (B10) to (B12) when n is replaced by 1/2 and r is computed from equation (B9).

The effects of internal rings in sandwich cylinders and of eccentric edge loading are not included in the preceding equations.

APPENDIX C

THERMAL PROTECTION ANALYSES

In performing the necessary thermal protection analyses to obtain the preliminary mass estimates of the multiwall and carbon dioxide concepts, approximate relations were used to compute the thermal conductivity of the multiwall sandwich and the thermal protection masses for the carbon dioxide concept. This appendix presents the approximate relations used in the thermal protection analyses.

Multiwall Concept

In the analyses of the multiwall concept, heat is transferred through a sandwich by one or combinations of the following modes of heat transfer: metal conduction, gas conduction, convection, and radiation. Thus, the apparent thermal conductivity is related to each mode of heat transfer. By assuming that the effect of each mode of heat transfer is independent, an approximate relation for the apparent thermal conductivity may be written in the form

$$k_a = \underbrace{k_m A_m\left(\frac{L}{Z}\right)}_{\text{Metal conduction}} + \underbrace{\frac{k_g\left(1 - A_m\right)}{1 - z/L}}_{\text{Gas conduction}} + \underbrace{\frac{LH_r\left(1 - A_m\right)}{j - 1}}_{\text{Radiation}} \tag{C1a}$$

$$k_a = \underbrace{k_m A_m\left(\frac{L}{Z}\right)}_{\text{Metal conduction}} + \underbrace{\frac{LH\left(1 - A_m\right)}{2(j - 1)}}_{\text{Gas convection}} + \underbrace{\frac{LH_r\left(1 - A_m\right)}{j - 1}}_{\text{Radiation}} \tag{C1b}$$

where $z < L$, and where H_r, the radiant heat transfer coefficient, is obtained from

$$H_r = 4\sigma F T_{ave}^3 \beta \tag{C2}$$

in which

$$F = \frac{1}{\frac{1}{f} + 2\left(\frac{1}{\epsilon} - 1\right)}, \quad T_{ave} = \frac{\left(T_H + T_C\right)}{2}$$

and β, the cube of the ratio of the mean temperature to the average temperature of the sandwich, is computed from

$$\beta = \frac{1 - \left(\frac{T_H - T_C}{T_H}\right) + 0.5\left(\frac{T_H - T_C}{T_H}\right)^2}{1 - \left(\frac{T_H - T_C}{T_H}\right) + 0.25\left(\frac{T_H - T_C}{T_H}\right)^2} \tag{C3}$$

APPENDIX C

For Grashof numbers less than 2000, equation (C1a) is used; for Grashof numbers greater than 2000, equation (C1b) is used. A comparison of the values of apparent thermal conductivity computed from equation (C1) and values obtained from experiments is shown in figure 14 in which a view factor of 0.7 and an average emittance of 0.85 were used in the calculations.

Carbon Dioxide Concept

In the thermal analysis of the carbon dioxide concept it is assumed that one-dimensional heat flow exists, that the tank radius is much greater than the insulation thickness, and that a steady-state condition exists. The thermal protection mass equals the sum of the insulation and coolant masses.

For the lower surface of the tank (see fig. 16), the insulation mass is given by

$$M_{ins} = \left[\rho_{ins} + \rho_F\left(1 - X_2/L\right)\right]L \tag{C4}$$

and the coolant mass, frost plus vaporized fuel mass charged to thermal protection, is given by

$$M_c = \frac{1}{L}\left[\frac{k_{ins}\left(T_o - T_s\right)\tau}{2(X/L)\Delta h_F} - \frac{k_{F,ins}\left(T_s - T_v\right)\tau}{2(1 - X/L)\Delta h_F} + \frac{k_{F,ins}\left(T_s - T_v\right)\tau}{(1 - X/L)\Delta h_{fu}}\right] \tag{C5}$$

in which

$$\Delta h_F = c_{p,F}\left(T_s - T_{F,I}\right) + \Delta h_s + \tfrac{1}{2}c_{p,g}\left(T_o - T_s\right)$$

where $T_{F,I}$ is the initial temperature of the frost at X/L. In deriving equation (C5) it is assumed that the fuel remains in contact with the lower tank wall during the powered ascent period and that frost sublimation ceases instantaneously at time τ. The value of (X/L) used in equation (C5) is obtained from

$$\frac{X}{L} = \frac{1}{2}\left(\frac{X_1}{L} + \frac{X_2}{L}\right) \tag{C6}$$

in which

$$\frac{X_1}{L} = \frac{1}{1 + \dfrac{k_{F,ins,G}\left(T_s - T_v\right)}{k_{ins,G}\left(T_{o,G} - T_s\right)}} \tag{C7}$$

$$\frac{X_2}{L} = \frac{1}{1 + \dfrac{k_{F,ins}\left(T_s - T_v\right)}{k_{ins}\left(T_o - T_s\right)}} \tag{C8}$$

APPENDIX C

The value of L used in computing M_{ins} and M_c is given by

$$L = \sqrt{\left[\frac{k_{ins}(T_o - T_s)\tau}{\rho_F(X/L)\Delta h_F} - \frac{k_{F,ins}(T_s - T_v)\tau}{\rho_F(1 - X/L)\Delta h_F}\right]\frac{1}{\left(\frac{X_2}{L} - \frac{X_1}{L}\right)}} \tag{C9}$$

For the upper surface of the tank, the insulation mass is given by equation (C4) and the coolant mass by

$$M_c = \frac{1}{L}\left[\frac{k_{ins}(T_o - T_s)\tau}{2(X/L)\Delta h_F} - \frac{k_{F,ins}(T_s - T_t)\tau}{2(1 - X/L)\Delta h_F}\right] \tag{C10}$$

Since the upper tank wall does not remain in contact with the fuel during the powered ascent period and its temperature remains below -110° F (195° K), the heat flow to the fuel was neglected in deriving equation (C10). The value of (X/L) used in equation (C10) is obtained from equation (C6) in which (X_2/L) is given by

$$\frac{X_2}{L} = \frac{1}{1 + \frac{k_{F,ins}(T_s - T_{t,f})}{k_{ins}(T_o - T_s)}} \tag{C11}$$

in which $T_{t,f}$ is selected at some value less than T_s based on frost coolant requirements for the time period beyond the powered flight time τ. The average temperature of the tank is computed from

$$T_t = T_s + \frac{(1 - X/L)M_t{}^2c_{p,t}{}^2(T_{t,f} - T_v)^2}{2\left(\frac{X_2}{L} - \frac{X_1}{L}\right)k_{F,ins}\tau\rho_F\Delta h_F}$$

$$- \sqrt{\frac{(1 - X/L)^2M_t{}^4c_{p,t}{}^4(T_{t,f} - T_v)^4}{4\left(\frac{X_2}{L} - \frac{X_1}{L}\right)^2 k_{F,ins}{}^2\tau^2\rho_F{}^2\Delta h_F{}^2} + \frac{k_{ins}(T_o - T_s)(1 - X/L)^2W_t{}^2c_{p,t}{}^2(T_{t,f} - T_v)^2}{k_{F,ins}{}^2\tau\rho_F(X/L)\Delta h_F\left(\frac{X_2}{L} - \frac{X_1}{L}\right)}} \tag{C12}$$

and L is computed from equation (C9) with T_v being replaced by T_t. To obtain the minimum permissible thermal protection mass, $T_{t,f}$ is selected and the tank temperature is calculated for the period beyond time τ for various values of (X_1/L) until the allowable maximum tank temperature is achieved; then another value of $T_{t,f}$ is selected and the calculations are repeated until the minimum permissible M_{tp} is obtained.

APPENDIX C

Modified Carbon Dioxide Concept

The same assumptions that are made in the analysis of the carbon dioxide concept are used in the analysis of the modified carbon dioxide concept. The insulation and coolant masses for the lower surface of a wing or fuselage section are computed from equations (C4) to (C9).

For the upper surface of a fuselage or wing section, the insulation mass is computed from equation (C4). The quantity (X_2/L) is equal to 1.0 in all related calculations. The value of L used in equations (C4) and (C13) is computed from equation (C9) with τ and T_v being replaced by $\lambda\tau$ and T_t, respectively. The coolant mass, frost plus vaporized fuel mass charged to thermal protection, is computed from

$$M_c = \frac{1}{L}\left[\frac{k_{ins}(T_o - T_s)\lambda^2\tau}{2(X/L)\Delta h_F} - \frac{k_{F,ins}(T_s - T_t)\lambda^2\tau}{2(1 - X/L)\Delta h_F} + \frac{LH_r(T_t - T_v)\lambda\tau}{\Delta h_{fu}} + \frac{LH'_r(T'_t - T_v)(1 - \lambda)\tau}{\Delta h_{fu}}\right] \tag{C13}$$

where T_t is computed from equation (C12) with τ being replaced by $\lambda\tau$ and $T_{t,f}$ is replaced by the tank temperature at time $\lambda\tau$, which is equal to T_s. For the time period $\lambda\tau$ to τ the tank temperature is determined by finite difference calculations, and the average tank temperature for this time period is T'_t. To obtain minimum masses for the insulation and coolants it is necessary to plot the total mass against λ for various values of (X_1/L) greater than that value of equation (C7) and less than 1.0. However, a constraint is that the amount of frost deposited on the upper surface must be compatible, in terms of percentage of insulation thickness containing frost, with the amount deposited on the lower surface since the depositions are not independent.

A comparison of solutions obtained for the carbon dioxide concept and for the modified carbon dioxide concept from numerical analyses and the approximate mass analyses indicates that the masses predicted by the approximate analyses are about 10 percent greater than the masses obtained from numerical analyses.

APPENDIX D

MULTIWALL SANDWICH EXPERIMENTS

Multiwall sandwich panels were subjected to noise, thermal conductivity, and thermal cycling tests.

Noise Test

A multiwall sandwich panel was tested under random noise to determine the effect of the environment on the panel. A description of the 12-inch-diameter unheated airjet utilized to perform this test is presented in reference 10. The multiwall panel was subjected to a random noise level of 162 decibels for 90 minutes. The panel did not exhibit any visible signs of damage after the test.

Apparent Thermal Conductivity Test

The thermal conductivities of two multiwall panels were obtained experimentally to determine the validity of the analytical method used in this paper to determine apparent thermal conductivity. A drawing of the multiwall panel used in the test is shown in figure 13. The apparatus utilized to perform the thermal conductivity test is described in reference 11. The panel was heated by quartz-tube lamps mounted above the panel. A 1-inch (2.54-cm) thick layer of insulation was placed beneath the test panel. The temperatures on the hot face of the panel, at the interface, and on the cold face of the insulation were measured with the aid of thermocouples. The steady-state temperature for the hot face of the panel was varied in increments from about 500 to 2000° F (530 to 1370° K). The apparent thermal conductivity of the panel was obtained from

$$k_a = k_{ins}\left(\frac{\Delta T_{ins}}{\Delta T_p}\right)\frac{L_p}{L_{ins}} \tag{D1}$$

The data recorded are shown as table II. A plot of the apparent thermal conductivity determined experimentally and analytically (appendix C) is shown in figure 14.

Thermal Cycling Test

The thermal cycling test was performed on a multiwall sandwich panel to determine the effect of thermal stress on the outer face sheet. The panel tested was 1 by 12 by 12 inches (2.5 by 30.5 by 30.5 cm) and consisted of six dimpled and seven nondimpled layers of light-gage stainless steel. The test was performed in the same facility used to perform the apparent thermal conductivity test. The hot face of the panel was raised from room temperature to approximately 1775° F (1240° K) in about 2 minutes, then the power

to the quartz-tube lamps was turned off and the panel was allowed to cool for 2 minutes. This procedure was repeated 25 times. After the first few cycles, the hot face of the panel cooled from about 1775° F (1240° K) to approximately 350° F (450° K) during the 2-minute cooling period. After 25 cycles the outer face sheet of the panel was still attached to the sandwich core. Several welds between the first and second core layers at one corner of the sandwich were broken during the test. In preparing the panel for test, it was noted that the pitch of the first core layer was slightly different from the pitch of the second core layer, which caused the dimples of the two layers to be out of alinement at the corners of the panel. Thus, some of the welds between the two core layers were abnormally weak. The effect of thermal cycling on the multiwall sandwich panel could not be fully determined.

APPENDIX E

CARBON DIOXIDE FROST DENSITY EXPERIMENTS

The cryodepositing of CO_2 frost in the voids of a low density insulation was performed to determine general conditions for CO_2 frost deposition and frost density. In addition, the prevention of cryopumping of air into the insulation space was an important test requirement.

The basic test apparatus for cryodepositing CO_2 frost is shown in figure 17. A removable cylindrical can containing fibrous insulation at a density of 6.5 lbm/ft^3 (104 kg/m^3) was sealed in a well which was installed in a cubical tank. Air was purged from the well space with helium gas. Helium pressure in the well was maintained at approximately 1 psig (6.9 kN/m^2) to prevent air from being cryopumped into the insulation space. A flow of CO_2 gas was initiated shortly after liquid nitrogen began flowing into the tank. The tank was filled with liquid nitrogen in approximately 1 hour. Test conditions were maintained for approximately 6 hours after which time the weight and volume of CO_2 frost were measured.

The test results indicated that the density of the CO_2 frost deposited was a function of the flow rate of CO_2 gas. A CO_2 gas flow of 3 ft^3/hr-ft^2 (254 cm^3/s-m^2) gave a frost density of approximately 30 lbm/ft^3 (481 kg/m^3) and a deposition rate of about 0.12 in./hr (0.846 μm/s). With no helium gas in the insulation space, CO_2 ice formed within the voids of the insulation regardless of the flow rate of CO_2 gas. The density of the CO_2 ice was approximately 100 lbm/ft3 (1.602 Mg/m3).

REFERENCES

1. Frick, C. W.; and Strand, T.: Recoverable Air-Breathing Boosters – Analysis of Their Potentialities. Aerospace Eng., vol. 20, no. 2, Feb. 1961, pp. 22-23, 66-70.

2. Gregory, Thomas J.; Petersen, Richard H.; and Wyss, John A.: Performance Trade-Offs and Research Problems for Hypersonic Transports. Paper No. 64-605, Am. Inst. Aeron. Astronaut., Aug. 1964.

3. Mechtly, E. A.: The International System of Units – Physical Constants and Conversion Factors. NASA SP-7012, 1964.

4. Rainey, Robert W.: Working Charts for Rapid Prediction of Force and Pressure Coefficients on Arbitrary Bodies of Revolution by Use of Newtonian Concepts. NASA TN D-176, 1959.

5. Anthony, Frank M.: Analytical Evaluation of Actively Cooled Modified Monocoque Structural Sandwich Concepts. Rept. No. 2225-900201 (Contract No. AF33(615)-1867), Bell Aerosystems Co., Nov. 1964.

6. Peterson, James P.: Weight-Strength Studies of Structures Representative of Fuselage Construction. NACA TN 4114, 1957.

7. Johnson, Aldie E., Jr.; and Semonian, Joseph W.: A Study of the Efficiency of High-Strength, Steel, Cellular-Core Sandwich Plates in Compression. NACA TN 3751, 1956.

8. Seide, Paul; and Stowell, Elbridge Z.: Elastic and Plastic Buckling of Simply Supported Solid-Core Sandwich Plates in Compression. NACA Report 967, 1950. (Supersedes NACA TN 1822.)

9. Stein, Manuel; and Mayers, J.: Compressive Buckling of Simply Supported Curved Plates and Cylinders of Sandwich Construction. NACA TN 2601, 1952.

10. Edge, Philip M., Jr.: Random-Noise Testing of Aircraft and Missile Components With the Aid of a Laboratory Air Jet. Shock, Vib. Assoc. Environments, Bull. No. 27, Pt. II, U.S. Dept. Defense, June 1959, pp. 169-174.

11. Wichorek, Gregory R.; and Stein, Bland A.: Experimental Investigation of Insulating Refractory-Metal Heat-Shield Panels. NASA TN D-1861, 1964.

TABLE I.- PRELIMINARY UNIT-AREA MASSES FOR MULTIWALL AND CARBON DIOXIDE CONCEPTS

(a) Multiwall concept

Location	Primary structure, lbm/ft^2 (kg/m^2)	Erosion shield and insulation, lbm/ft^2 (kg/m^2)	Boiloff, lbm/ft^2 (kg/m^2)	Total, lbm/ft^2 (kg/m^2)
Lower body	2.01 (9.81)	2.73 (13.3)	0.44 (2.15)	5.18 (25.3)
Upper body	2.01 (9.81)	1.14 (5.56)	.40 (1.95)	3.55 (17.3)
Lower wing	2.35 (11.5)	2.48 (12.1)	.62 (3.02)	5.45 (26.6)
Upper wing	2.58 (12.6)	1.14 (5.56)	.25 (1.22)	3.97 (19.4)

(b) Carbon dioxide concept

Location	Primary structure, lbm/ft^2 (kg/m^2)	Insulation, lbm/ft^2 (kg/m^2)	Frost, lbm/ft^2 (kg/m^2)	Boiloff, lbm/ft^2 (kg/m^2)	Tank, lbm/ft^2 (kg/m^2)	Total, lbm/ft^2 (kg/m^2)
Lower body	2.67 (13.0)	0.23 (1.12)	0.47 (2.30)	0.76 (3.70)	2.25 (11.0)	6.38 (31.2)
Upper body	2.67 (13.0)	.34 (1.66)	.42 (2.05)	0 (0)	2.25 (11.0)	5.68 (27.7)

(c) Modified carbon dioxide concept

Location	Primary structure, lbm/ft^2 (kg/m^2)	Erosion shield and insulation, lbm/ft^2 (kg/m^2)	Frost, lbm/ft^2 (kg/m^2)	Boiloff, lbm/ft^2 (kg/m^2)	Total, lbm/ft^2 (kg/m^2)
Lower body	2.50 (12.2)	1.35 (6.59)	1.05 (5.12)	1.66 (8.10)	6.56 (32.0)
Upper body	2.50 (12.2)	1.20 (5.85)	.35 (1.71)	.29 (1.42)	4.34 (21.2)
Lower wing	3.05 (14.9)	1.34 (6.54)	1.04 (5.07)	1.65 (8.05)	7.08 (34.6)
Upper wing	3.25 (15.9)	1.04 (5.07)	.24 (1.17)	.35 (1.71)	4.88 (23.8)

TABLE II.- THERMAL CONDUCTIVITY DATA

Specimen mean temperature, ^{o}F (^{o}K)	Specimen temperature difference, ^{o}F (^{o}K)	Insulation mean temperature, ^{o}F (^{o}K)	Insulation temperature difference, ^{o}F (^{o}K)	Insulation thermal conductivity, Btu/hr-ft-^{o}F (mW/m-^{o}K)
1878 (1300)	207 (115)	1228 (938)	1092 (606)	0.105 (181)
1645 (1170)	203 (113)	1073 (853)	942 (524)	.082 (142)
1317 (984)	200 (111)	820 (711)	795 (441)	.059 (102)
1288 (970)	185 (103)	803 (702)	785 (436)	.057 (98.6)
1095 (864)	170 (94.4)	683 (636)	655 (364)	.049 (84.7)
1023 (824)	165 (91.6)	650 (616)	581 (323)	.047 (81.1)
775 (686)	150 (83.3)	450 (506)	500 (278)	.037 (63.9)
761 (679)	148 (82.2)	470 (516)	490 (272)	.036 (62.2)
725 (658)	110 (61.0)	450 (506)	440 (244)	.037 (63.9)
545 (548)	80 (44.5)	350 (450)	310 (172)	.033 (57.1)
485 (535)	94 (52.2)	324 (436)	228 (126)	.032 (55.3)
472 (518)	67 (37.2)	318 (433)	241 (134)	.032 (55.3)

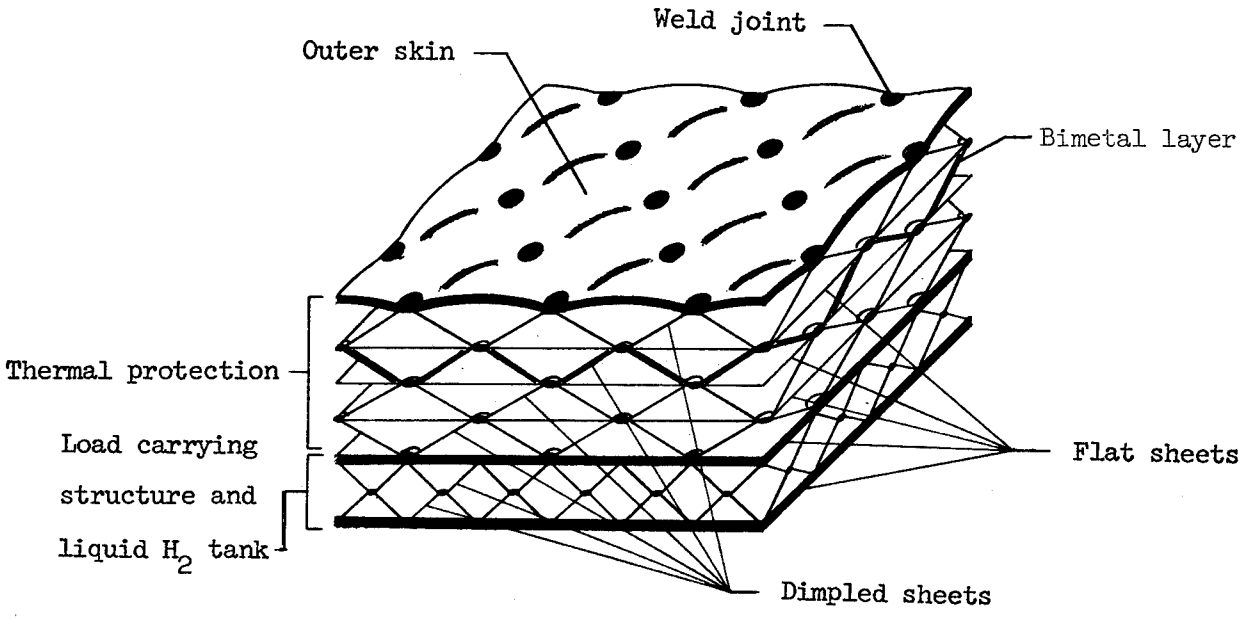

(a) Multiwall sandwich panel.

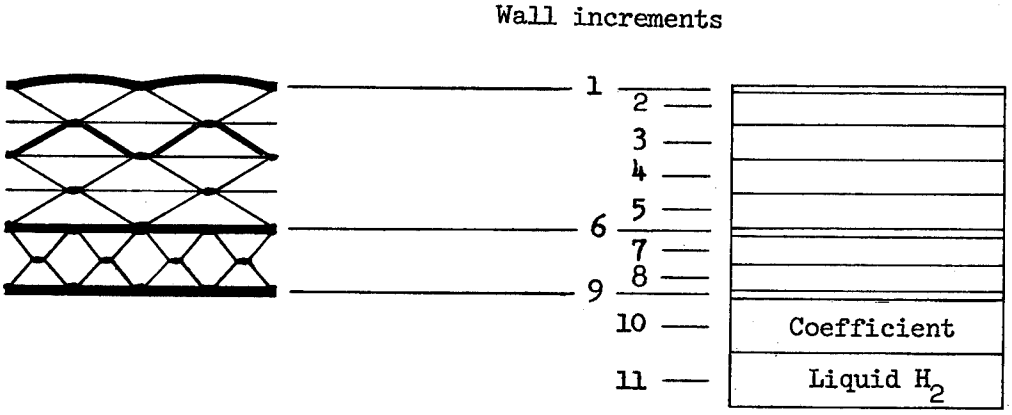

(b) Mathematical model.

Figure 1.- Multiwall concept.

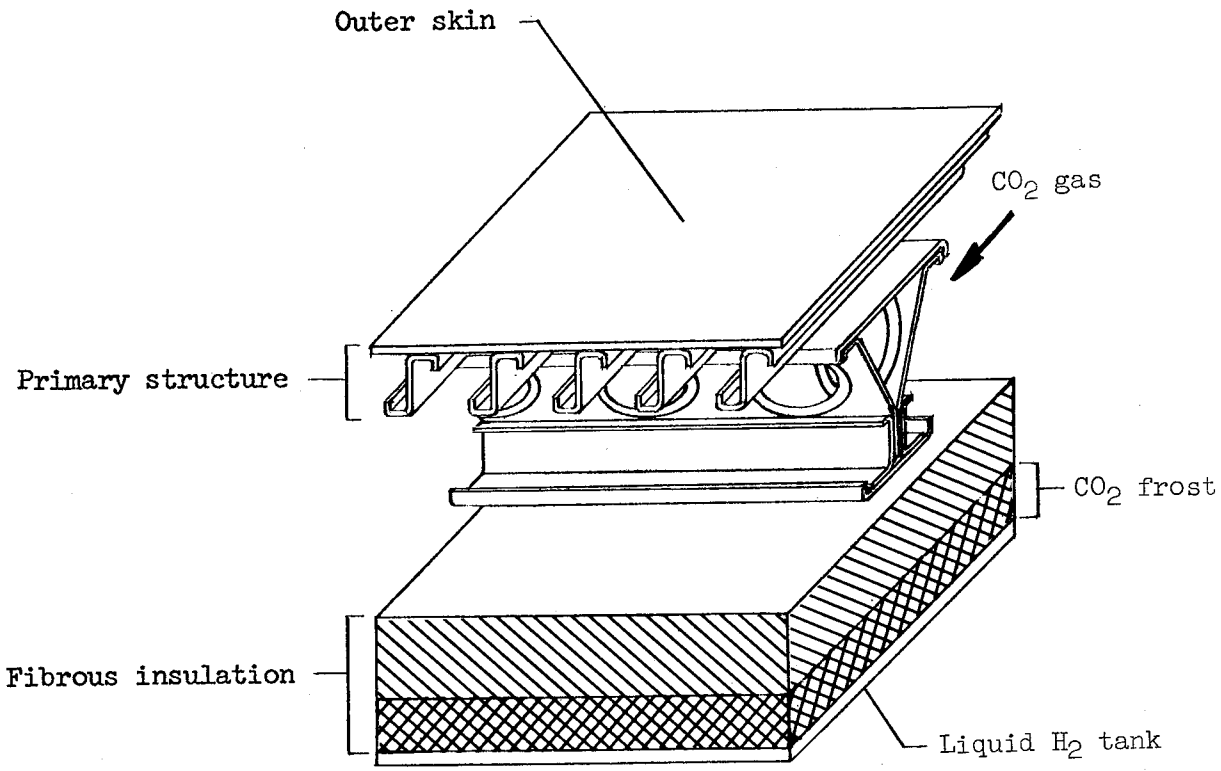

Figure 2.- Carbon dioxide concept.

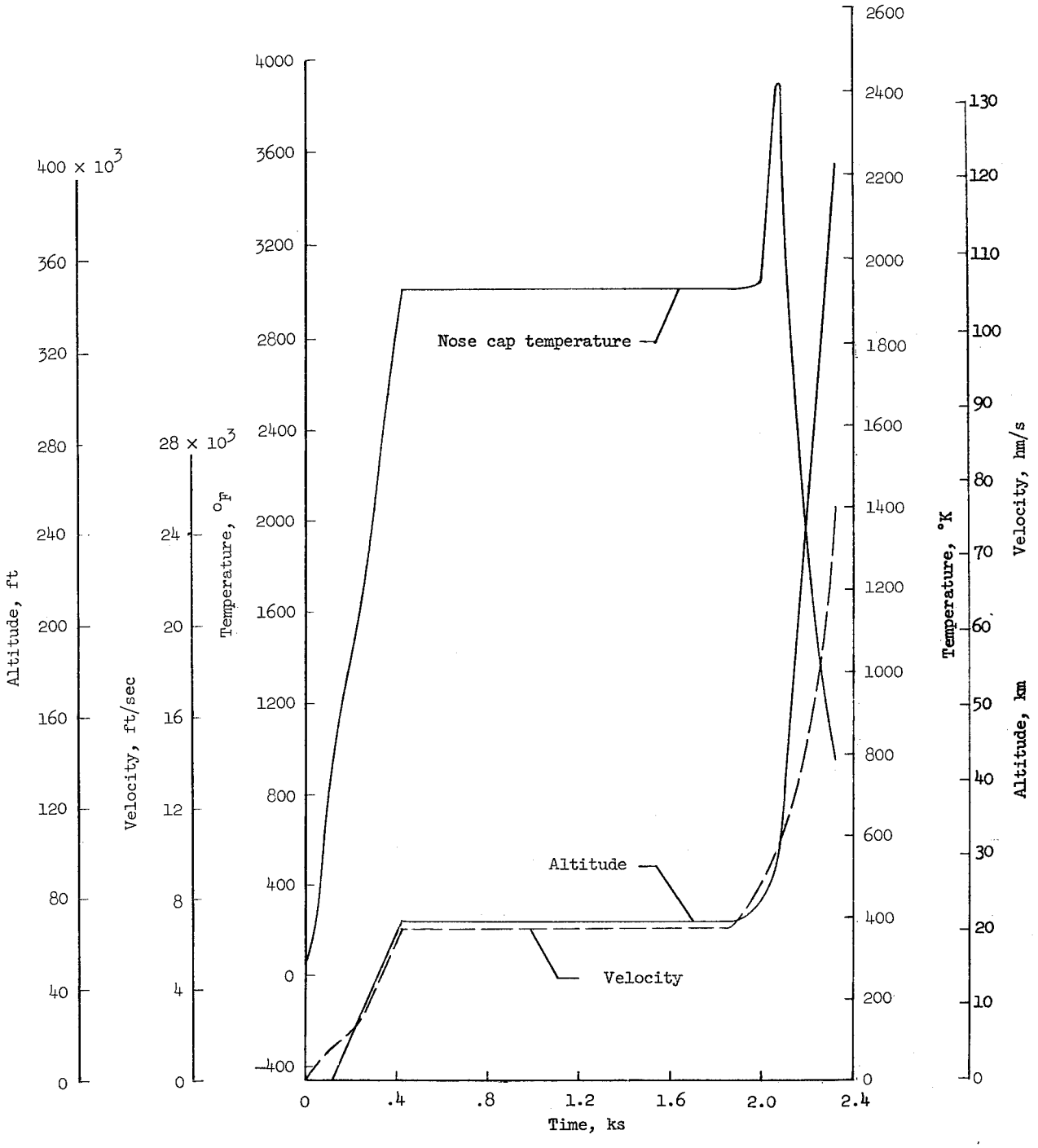

Figure 3.- Ascent trajectory used in the preliminary mass analyses of the multiwall concept.

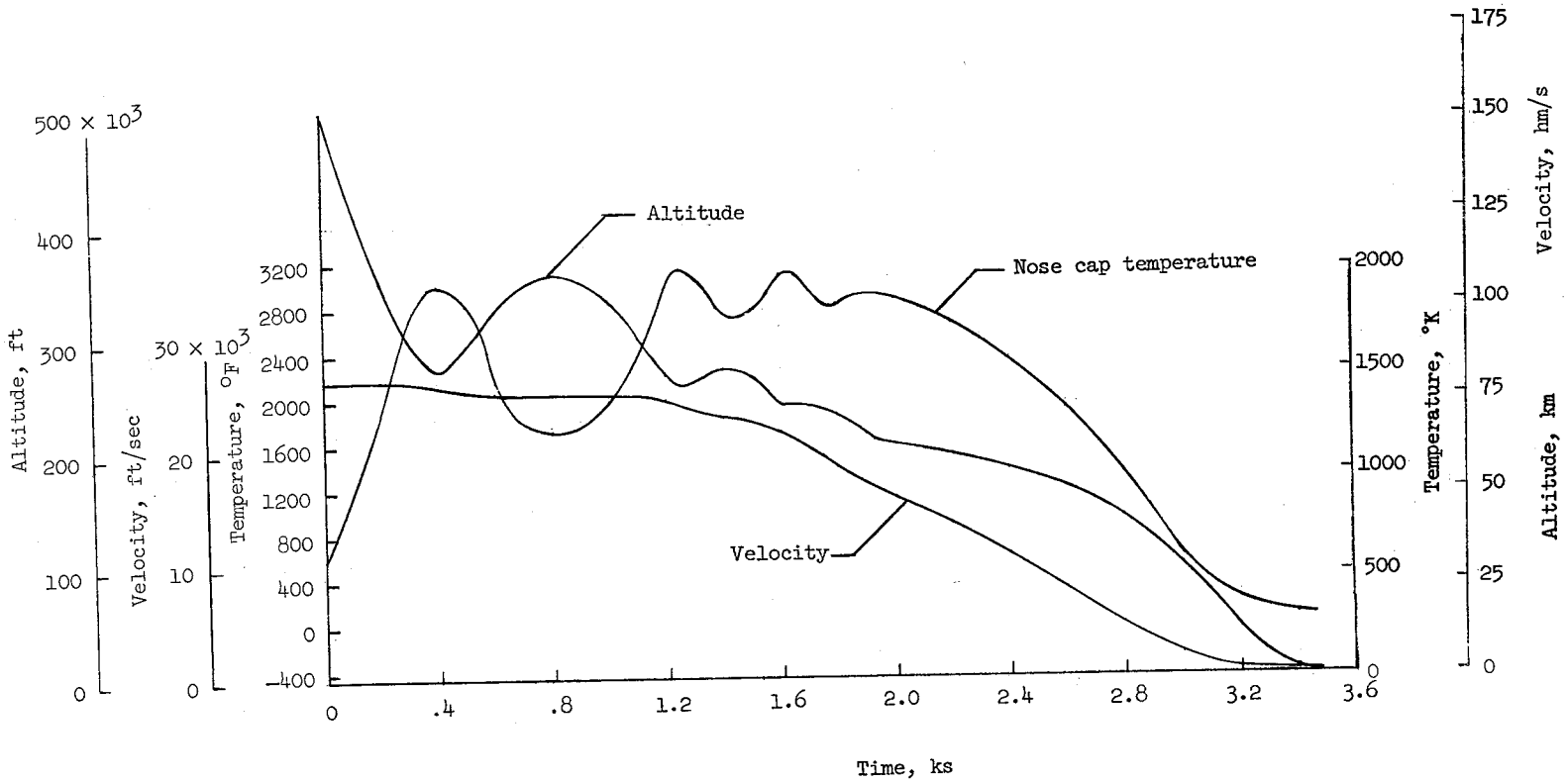

Figure 4.- Reentry trajectory used in the preliminary mass analyses of the multiwall concept.

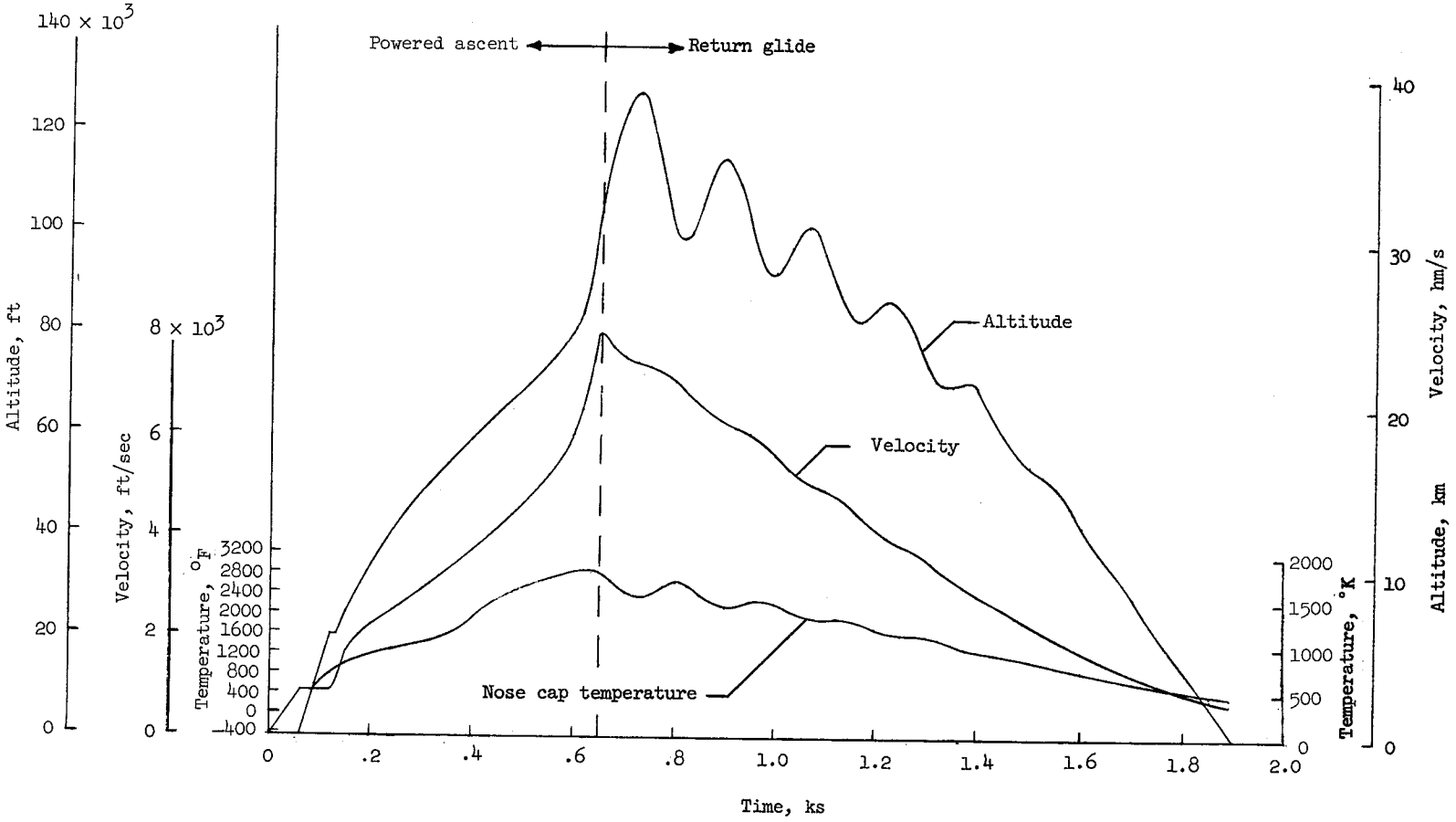

Figure 5.- Ascent and return glide trajectory used in the preliminary mass analyses of the carbon dioxide concept.

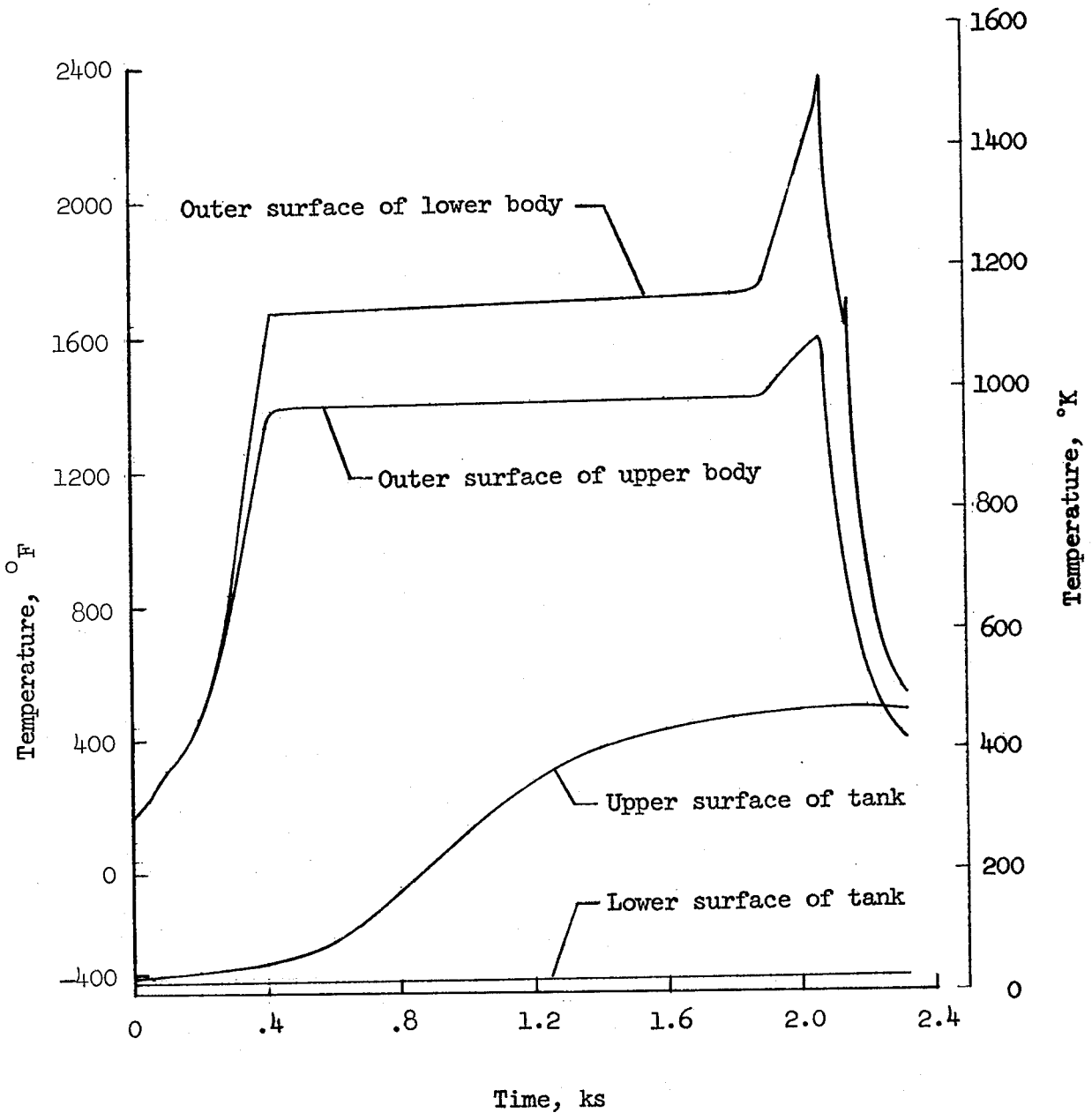

Figure 6.- Temperature history of multiwall concept during ascent.

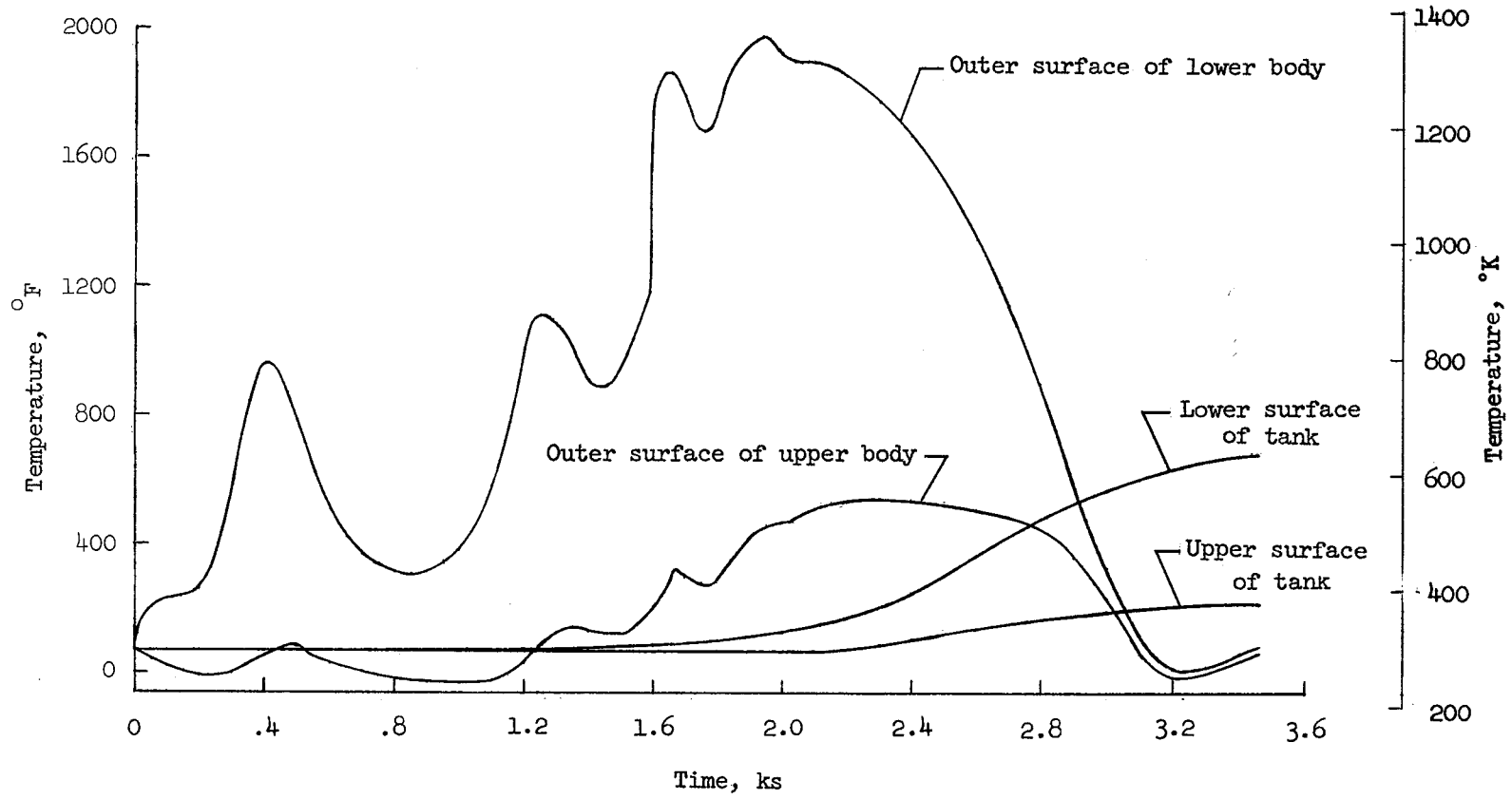

Figure 7.- Temperature history of multiwall concept during reentry.

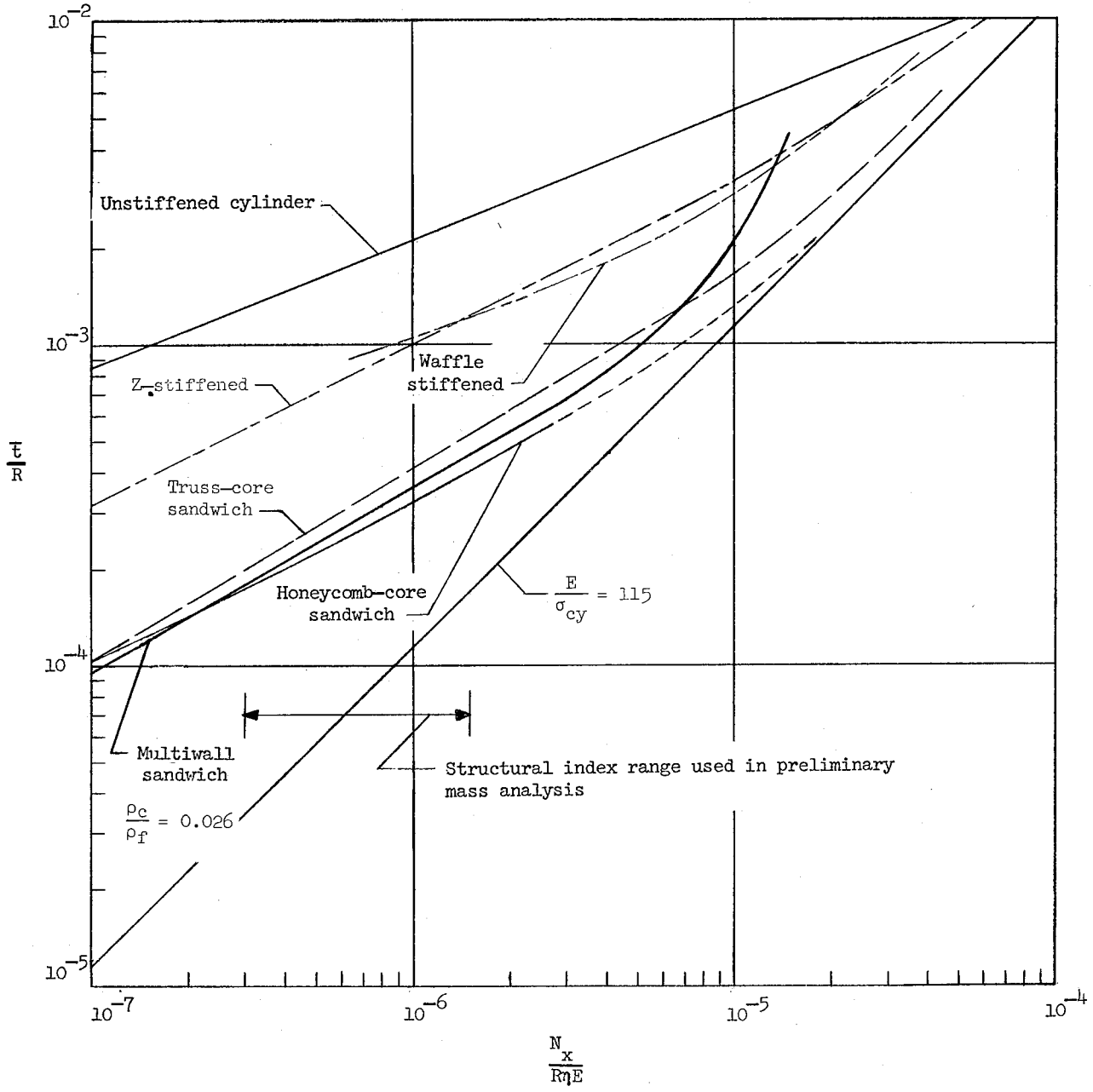

Figure 8.- Structural index curves for cylindrical shells of various constructions subjected to axial compression.

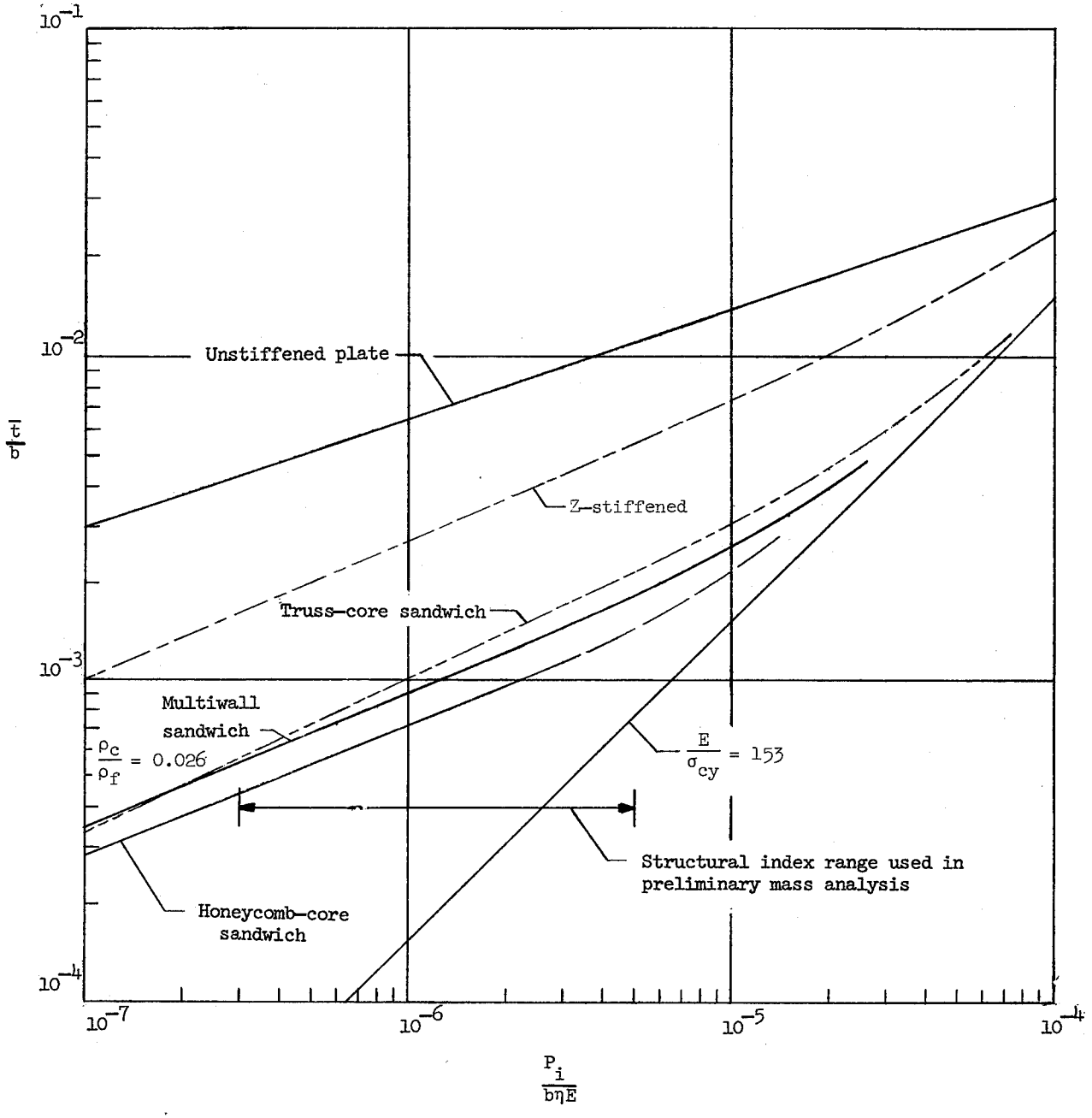

Figure 9.- Structural index curves for flat plates of various constructions subjected to edge compression.

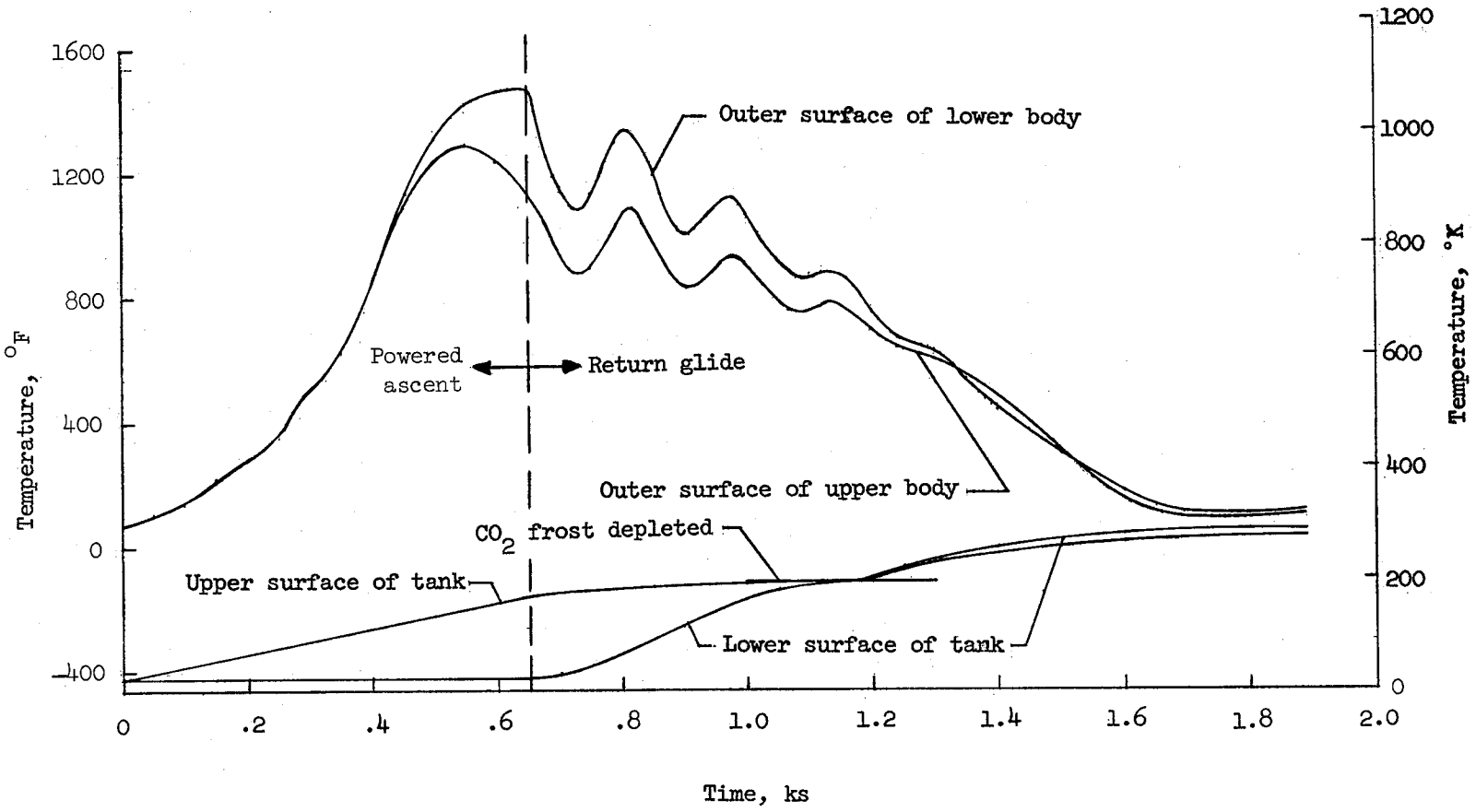

Figure 10.- Temperature history of carbon dioxide concept.

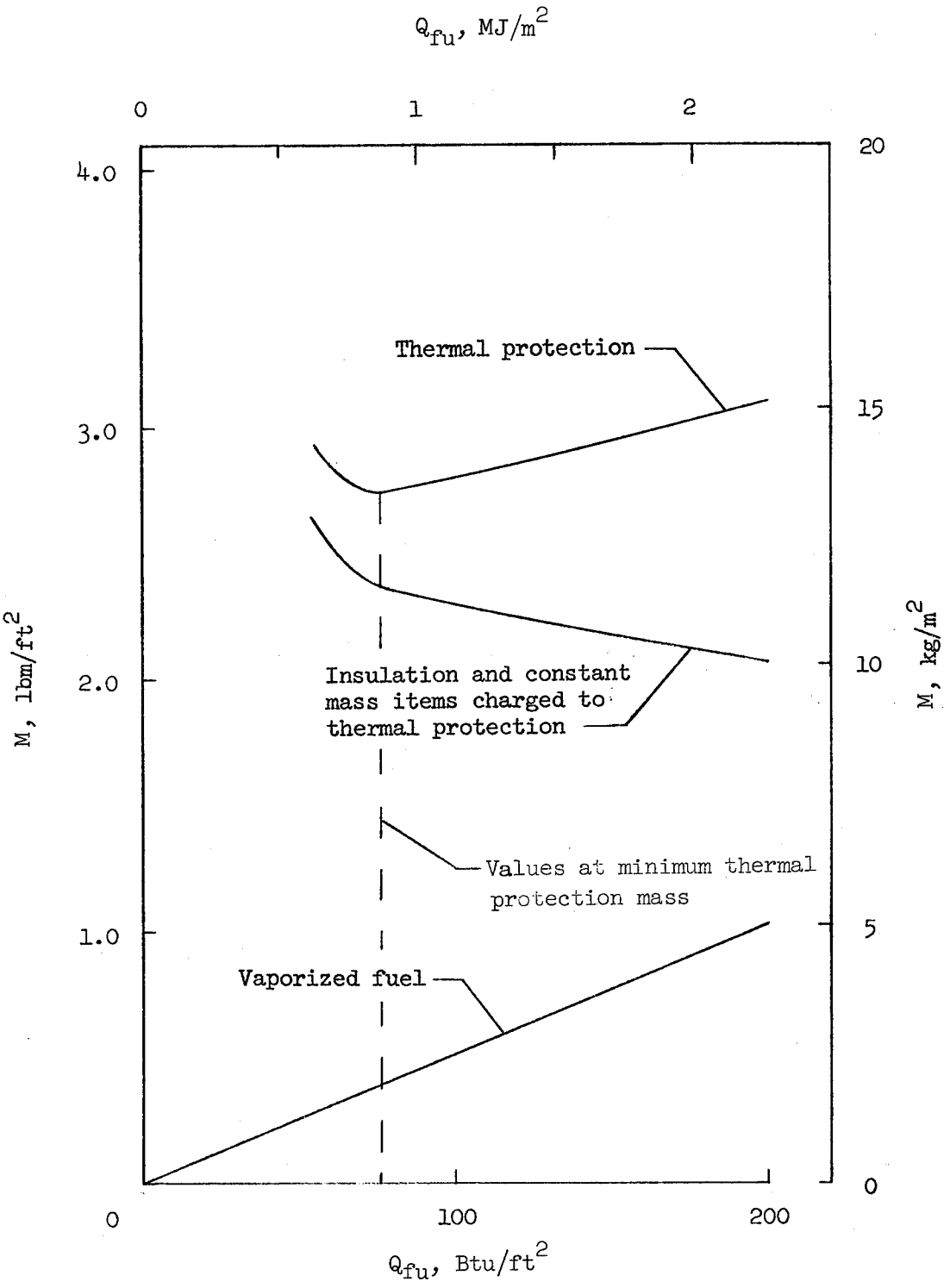

Figure 11.- Typical thermal protection mass curves.

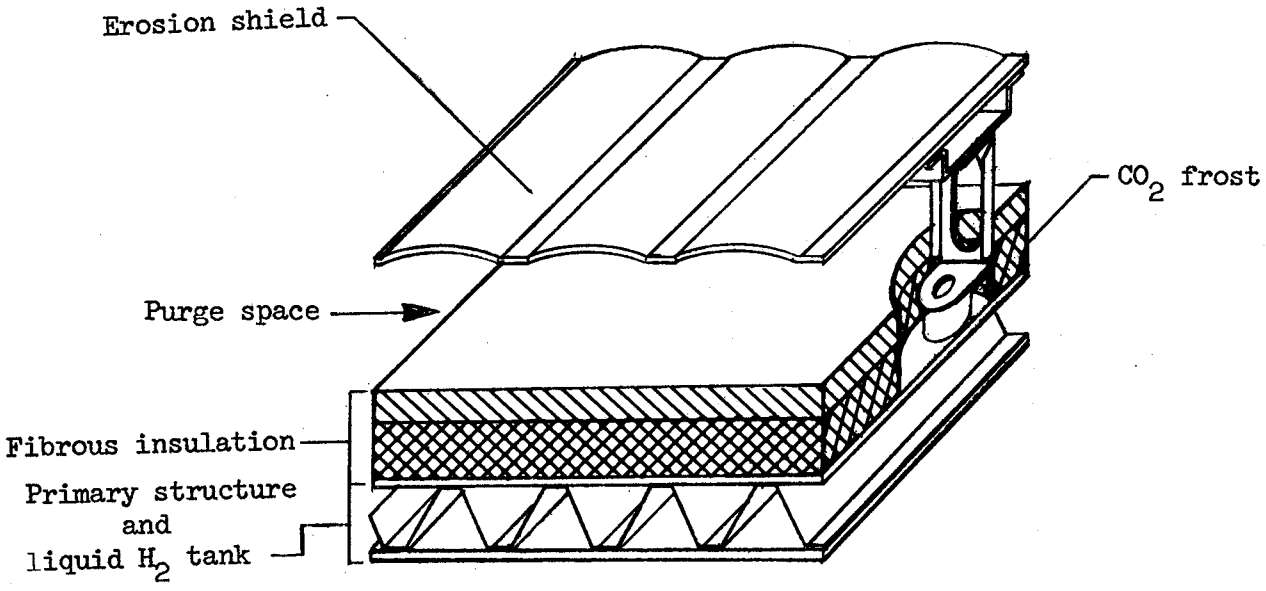

Figure 12.- Modified carbon dioxide concept.

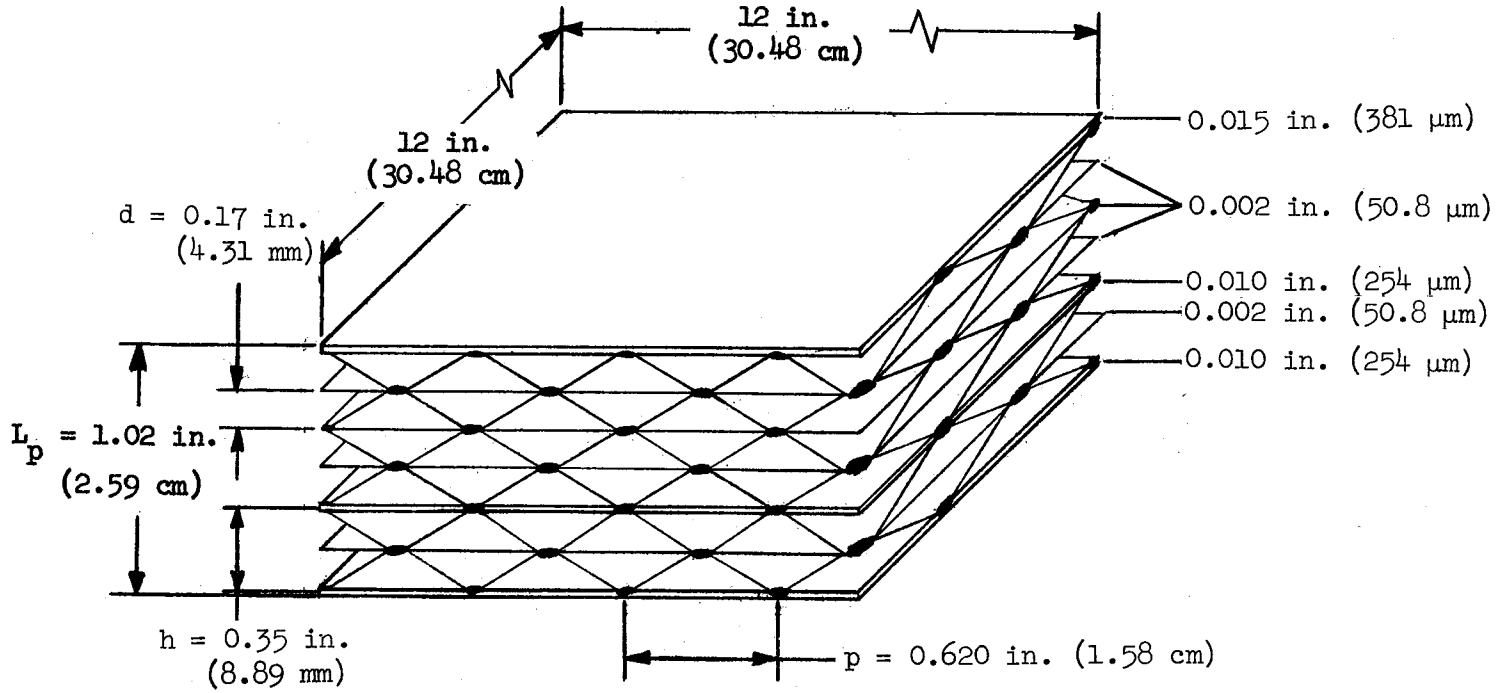

Figure 13.- Multiwall sandwich panel. (Dimpled sheets are 0.004 in. (102 μm) thick.)

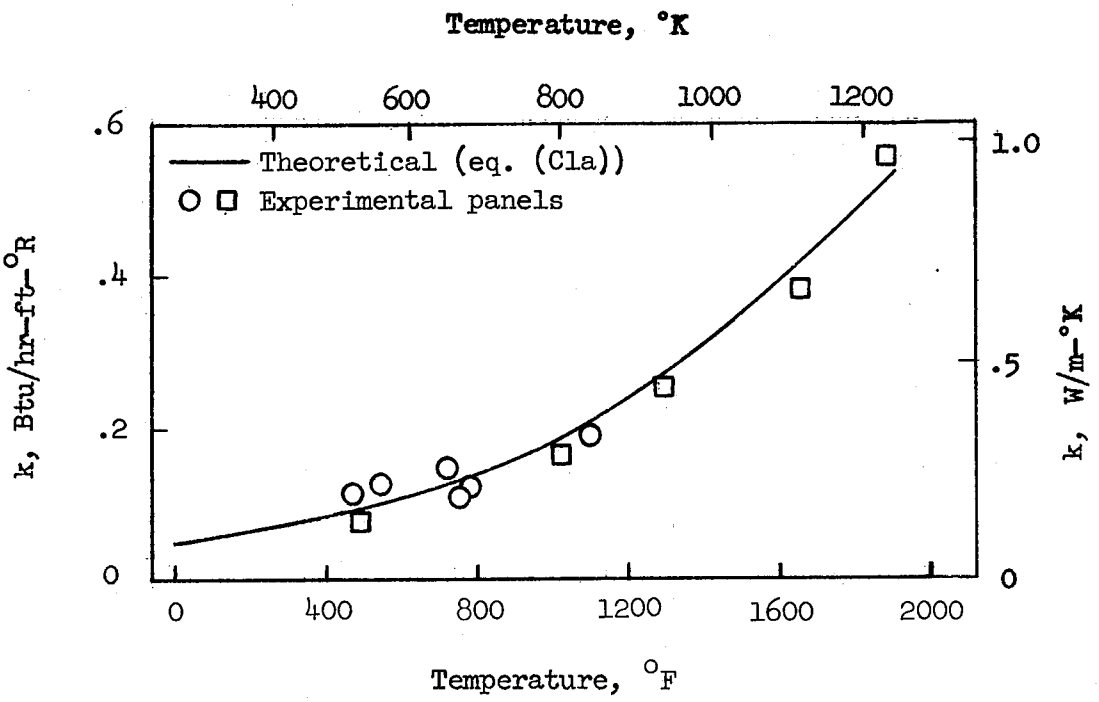

Figure 14.- Variation of apparent thermal conductivity with temperature for multiwall sandwich test panels.

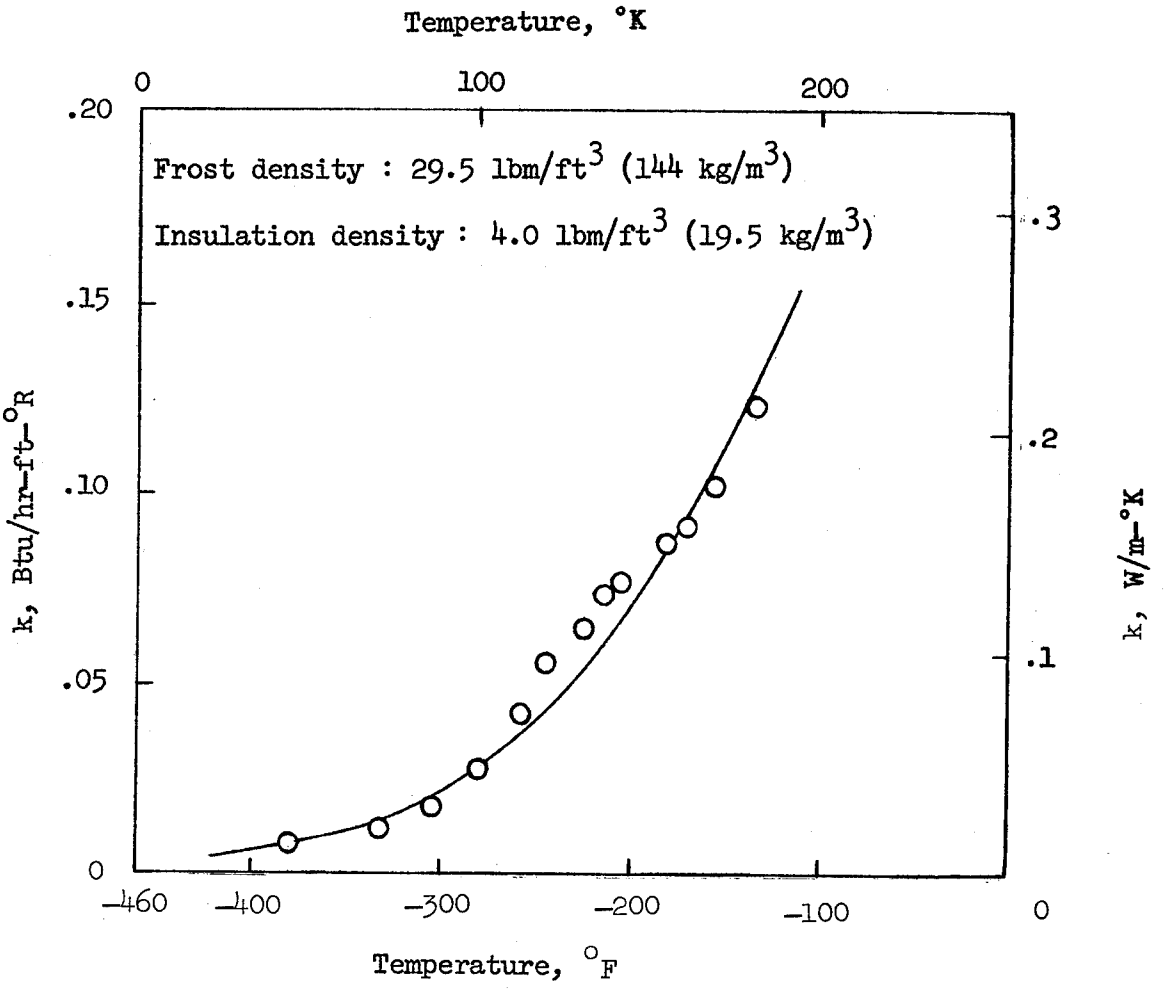

Figure 15.- Apparent thermal conductivity of CO_2 frost cryodeposited within a fibrous insulation.

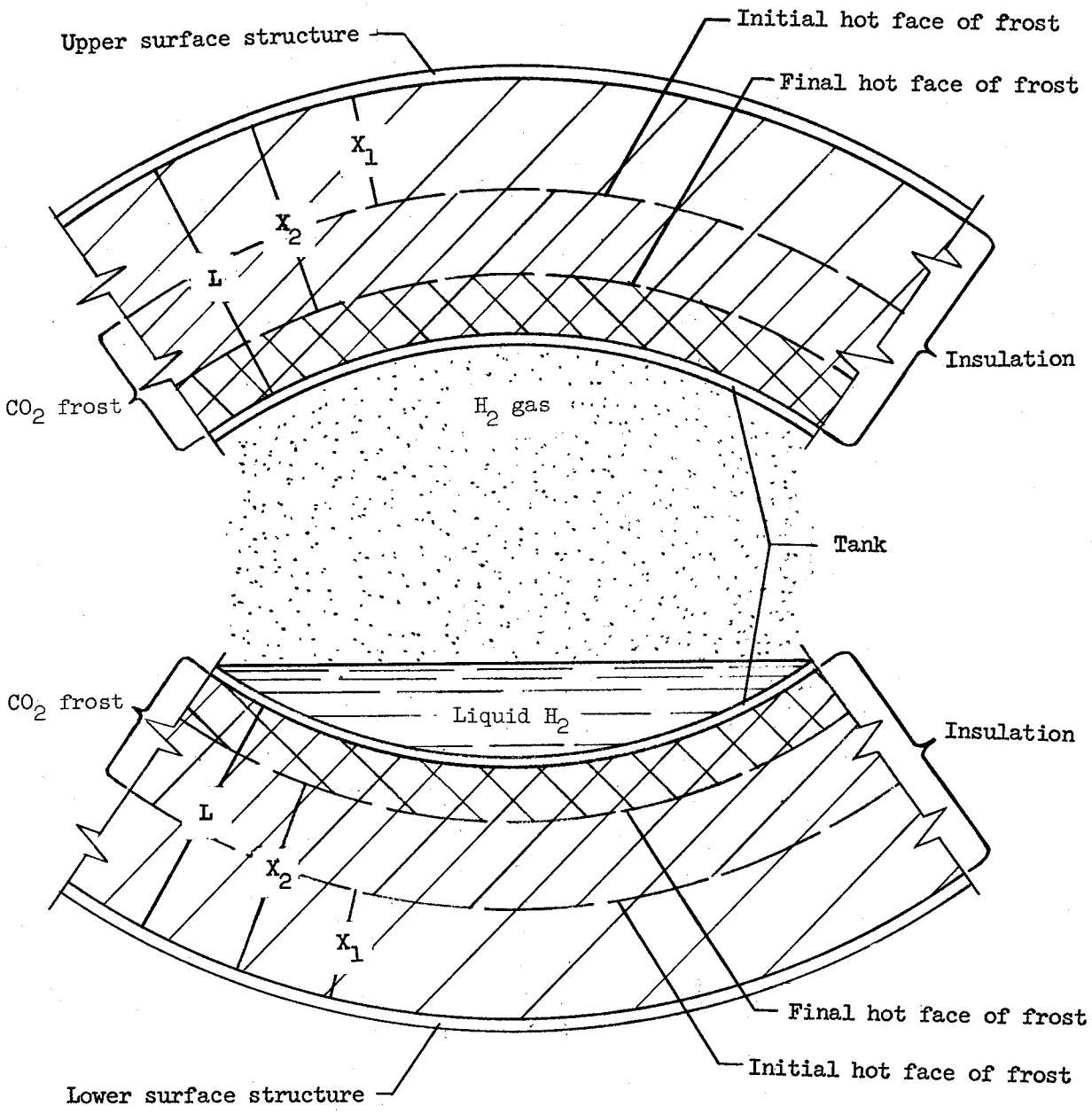

Figure 16.- Schematic of carbon dioxide system.

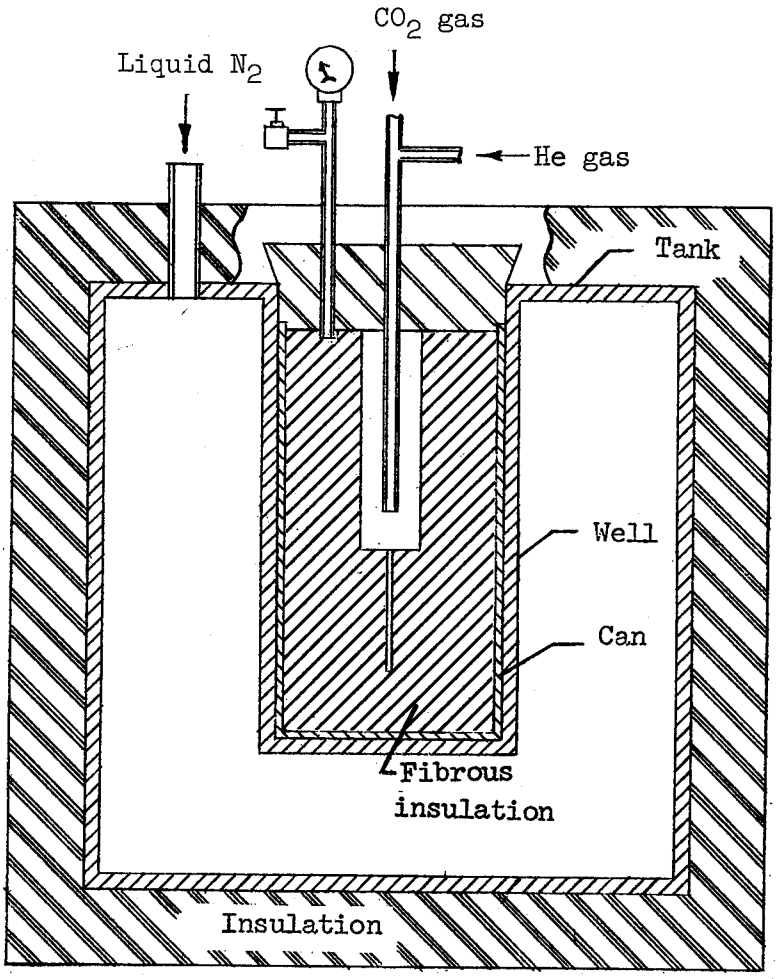

Figure 17.- Test apparatus for cryodepositing CO_2 frost.

NASA-Langley, 1966 L-4495

"The aeronautical and space activities of the United States shall be conducted so as to contribute . . . to the expansion of human knowledge of phenomena in the atmosphere and space. The Administration shall provide for the widest practicable and appropriate dissemination of information concerning its activities and the results thereof."

—NATIONAL AERONAUTICS AND SPACE ACT OF 1958

NASA SCIENTIFIC AND TECHNICAL PUBLICATIONS

TECHNICAL REPORTS: Scientific and technical information considered important, complete, and a lasting contribution to existing knowledge.

TECHNICAL NOTES: Information less broad in scope but nevertheless of importance as a contribution to existing knowledge.

TECHNICAL MEMORANDUMS: Information receiving limited distribution because of preliminary data, security classification, or other reasons.

CONTRACTOR REPORTS: Technical information generated in connection with a NASA contract or grant and released under NASA auspices.

TECHNICAL TRANSLATIONS: Information published in a foreign language considered to merit NASA distribution in English.

TECHNICAL REPRINTS: Information derived from NASA activities and initially published in the form of journal articles.

SPECIAL PUBLICATIONS: Information derived from or of value to NASA activities but not necessarily reporting the results of individual NASA-programmed scientific efforts. Publications include conference proceedings, monographs, data compilations, handbooks, sourcebooks, and special bibliographies.

Details on the availability of these publications may be obtained from:

SCIENTIFIC AND TECHNICAL INFORMATION DIVISION

NATIONAL AERONAUTICS AND SPACE ADMINISTRATION

Washington, D.C. 20546